Theoretical review on light meson and heavy hadron spectroscopy

Qiang Zhao

Theoretical Physics Division

Institute of High Energy Physics, Chinese Academy of Sciences

zhaoq@ihep.ac.cn

17th International Conference on Heavy Quarks and Leptons (HQL 2025), Peking University,

Sept. 15-19, 2025

中国科学院高能物理研究所

Institute of High Energy Physics, CAS

中国科学院

CHINESE ACADEMY OF SCIENCES

Some insights into the non-perturbative QCD phenomena

Qiang Zhao

Theoretical Physics Division

Institute of High Energy Physics, Chinese Academy of Sciences

zhaoq@ihep.ac.cn

17th International Conference on Heavy Quarks and Leptons (HQL 2025), Peking University,

Sept. 15-19, 2025

Outline

1. Hadrons beyond the conventional quark model
2. Vector charmonia probed in e^+e^- annihilations
3. Non-perturbative mechanism probed in heavy hadron hadronic weak decays
4. Summary

1. Hadrons beyond the conventional quark model

Exotics of Type-I:

J^{PC} are not allowed by $Q\bar{Q}$ configurations, e.g. $0^{--}, 1^{-+}$ …

- Direct observation

Exotics of Type-II:

J^{PC} are the same as $Q\bar{Q}$ configurations

- Outnumbering of conventional QM states?
- Peculiar properties?

"Exotics" of Type-III:

Leading kinematic singularity can cause measurable effects, e.g. the triangle singularity.

- What's the impact?
- How to distinguish a genuine state from kinematic effects?

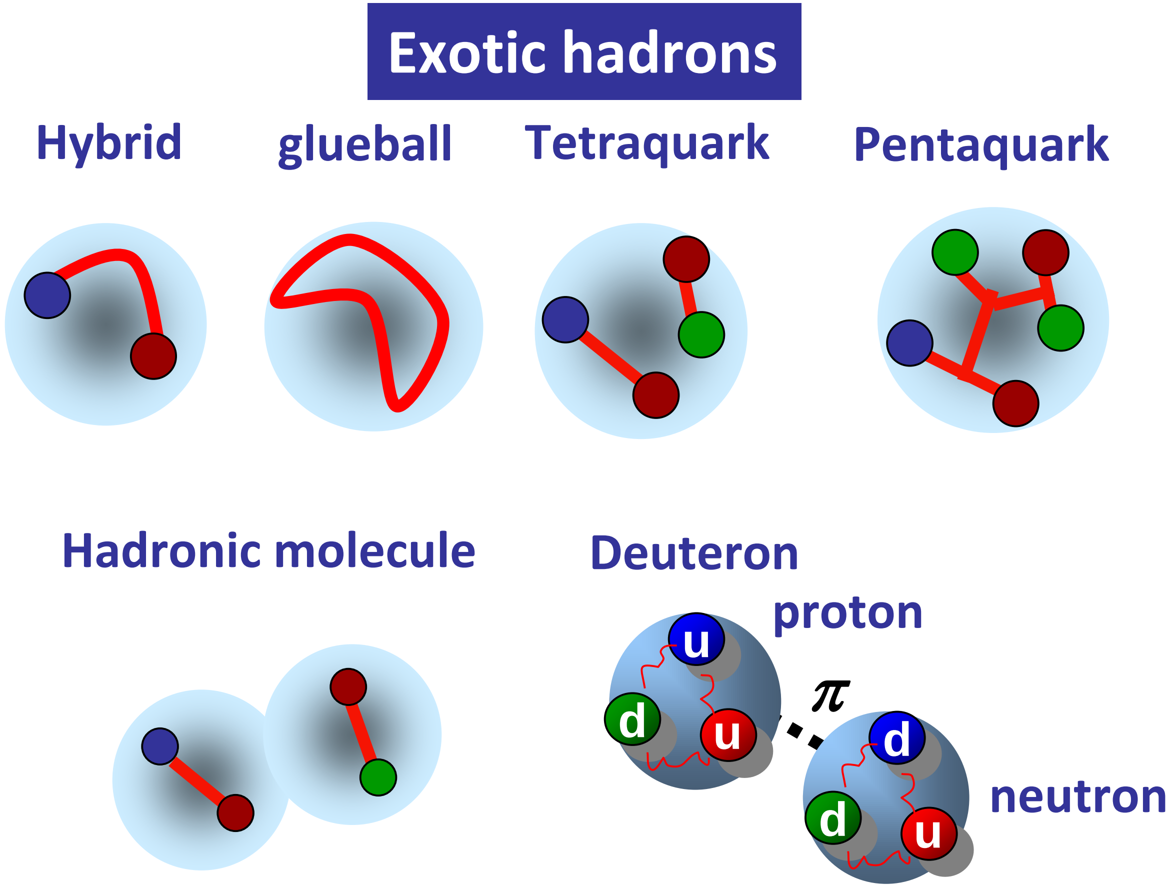

Evidence for QCD exotic states is a missing piece of knowledge about the Nature of strong QCD.

$q\bar{q}$ SU(3) flavor nonet: $\bar{3}\otimes 3 = 1 \oplus 8$

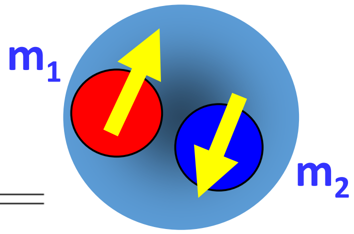

$n^{2s+1}\ell_J$	J^{PC}	$I=1$ $u\bar{d}$, $\bar{u}d$, $\frac{1}{\sqrt{2}}(d\bar{d}-u\bar{u})$	$I=\frac{1}{2}$ $u\bar{s}$, $d\bar{s}$; $\bar{d}s$, $\bar{u}s$	$I=0$ f'	$I=0$ f
1^1S_0	0^{-+}	π	K	η	$\eta'(958)$
1^3S_1	1^{--}	$\rho(770)$	$K^*(892)$	$\phi(1020)$	$\omega(782)$
1^3P_0	0^{++}	$a_0(1450)$	$K_0^*(1430)$	$f_0(1370, 1500, 1710)$	
1^1P_1	1^{+-}	$b_1(1235)$	K_{1B}[a]	$h_1(1415)$	$h_1(1170)$
1^3P_1	1^{++}	$a_1(1260)$	K_{1A}[a]	$f_1(1420)$	$f_1(1285)$
1^3P_2	2^{++}	$a_2(1320)$	$K_2^*(1430)$	$f_2'(1525)$	$f_2(1270)$
1^3D_1	1^{--}	$\rho(1700)$	$K^*(1680)$[b]	$\phi(2170)$[c]	$\omega(1650)$
1^1D_2	2^{-+}	$\pi_2(1670)$	$K_2(1770)$[a]	$\eta_2(1870)$	$\eta_2(1645)$
1^3D_3	3^{--}	$\rho_3(1690)$	$K_3^*(1780)$	$\phi_3(1850)$	$\omega_3(1670)$
1^3F_4	4^{++}	$a_4(1970)$	$K_4^*(2045)$	$f_4(2300)$	$f_4(2050)$
1^3G_5	5^{--}	$\rho_5(2350)$	$K_5^*(2380)$		
2^1S_0	0^{-+}	$\pi(1300)$	$K(1460)$	$\eta(1475)$[d]	$\eta(1295)$
2^3S_1	1^{--}	$\rho(1450)$	$K^*(1410)$[b]	$\phi(1680)$	$\omega(1420)$
2^3P_1	1^{++}	$a_1(1640)$	$K_1(1650)$		
2^3P_2	2^{++}	$a_2(1700)$	$K_2^*(1980)$	$f_2(1950)$[e]	$f_2(1640)$
2^1D_2	2^{-+}	$\pi_2(1880)$			
3^1S_0	0^{-+}	$\pi(1800)$	$K(1830)$		$\eta(1760)$

$a_1(1420)$?

$\eta(1405)$?

- Most of the observed low-lying states can be accommodated by the CQM
- Most of the higher states predicted by the CQM are still missing
- Deviations from the CQM are evident and need understanding
  - Scalar nonet below 1 GeV, $\sigma(600), \kappa(700), f_0(980), a_0(980)$.
  - Out-numbering of the CQM multiplets
  - Signals with exotic quantum numbers, e.g. $J^{PC} = 0^{--}, 1^{-+}, 2^{+-}, \ldots$
  - Special non-resonance structures, e.g. triangle singularity

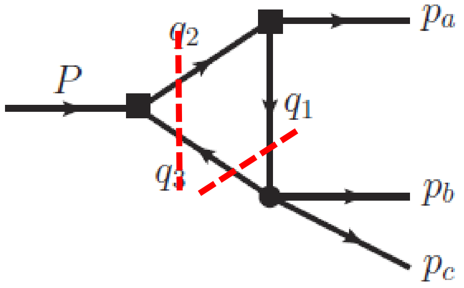

Ways to produce QCD exotics

e^+e^- annihilation

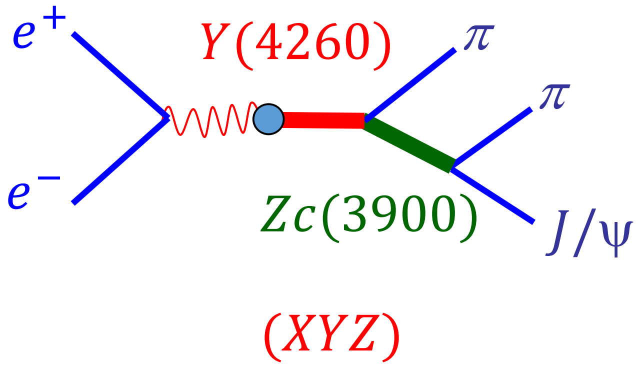

$\gamma\gamma$ scatterings

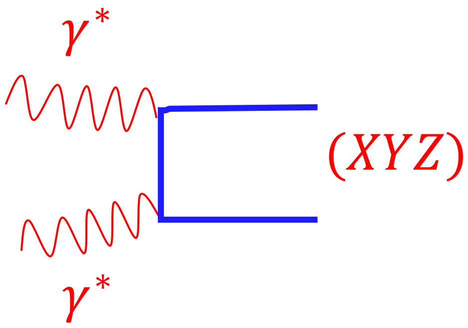

Hadron colli.

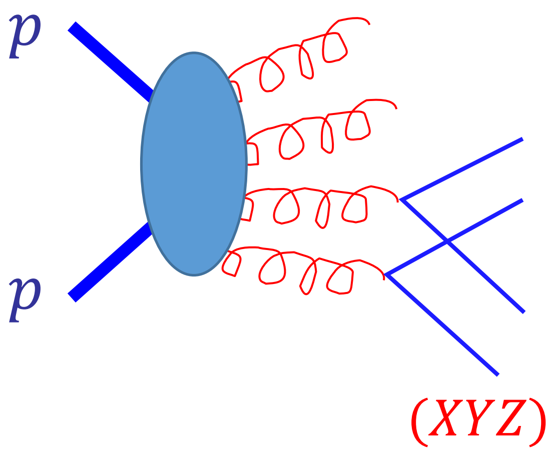

Weak decays

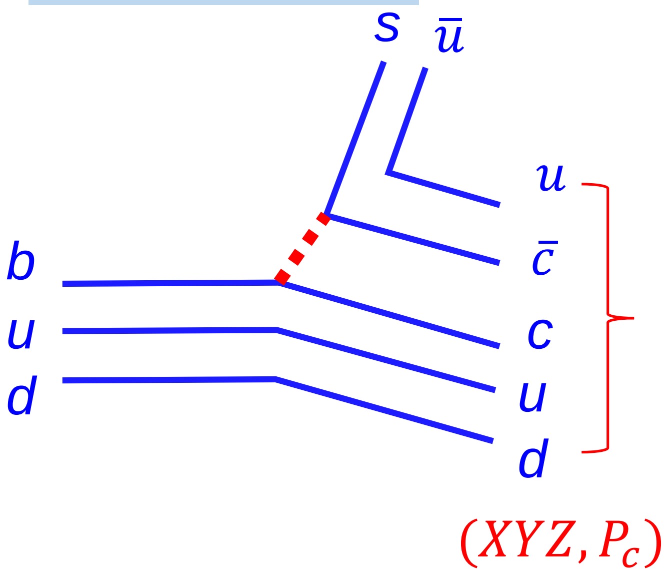

Hadron physics is a natural part of large science facilities.

Success of Quark Model:
Hadrons are made of quarks (antiquarks) as QCD color singlet

Hamiltonian in a non-relativistic quark model :

$$H = \left(\sum_{i=1}^{4} m_i + T_i\right) - T_G + \sum_{i<j} V_{ij}(r_{ij})$$

$$T_i = \frac{p_i^2}{2m_i}, \qquad V_{ij}(r_{ij}) = V_{ij}^{\rm OGE}(r_{ij}) + V_{ij}^{\rm Conf}(r_{ij}),$$

$$V_{ij}^{\rm Conf}(r_{ij}) = -\frac{3}{16}(\lambda_i \cdot \lambda_j) \cdot b r_{ij},$$

Potential smearing factor

$$V_{ij}^{\rm OGE} = \frac{\alpha_{ij}}{4}(\lambda_i \cdot \lambda_j)\left\{\frac{1}{r_{ij}} - \frac{\pi}{2} \cdot \frac{\sigma_{ij}^3 e^{-\sigma_{ij}^2 r_{ij}^2}}{\pi^{3/2}} \cdot \frac{4}{3m_i m_j}(\boldsymbol{\sigma}_i \cdot \boldsymbol{\sigma}_j)\right\}$$

Coulomb **Spin-spin correl.**

$$V_{ij}^{LS} = -\frac{\alpha_{ij}}{16}\frac{\lambda_i \cdot \lambda_j}{r_{ij}^3}\left(\frac{1}{m_i^2} + \frac{1}{m_j^2} + \frac{4}{m_i m_j}\right)\left\{\mathbf{L}_{ij} \cdot (\mathbf{S}_i + \mathbf{S}_j)\right\} - \frac{\alpha_{ij}}{16}\frac{\lambda_i \cdot \lambda_j}{r_{ij}^3}\left(\frac{1}{m_i^2} - \frac{1}{m_j^2}\right)\left\{\mathbf{L}_{ij} \cdot (\mathbf{S}_i - \mathbf{S}_j)\right\},$$

$$V_{ij}^{T} = -\frac{\alpha_{ij}}{4}(\lambda_i \cdot \lambda_j)\frac{1}{m_i m_j r_{ij}^3}\left\{\frac{3(\mathbf{S}_i \cdot \mathbf{r}_{ij})(\mathbf{S}_j \cdot \mathbf{r}_{ij})}{r_{ij}^2} - \mathbf{S}_i \cdot \mathbf{S}_j\right\}$$

- **Cornell potential model**
- **Godfrey-Isgur model**
- **A lot of recent developments …**

The connection between the quark model and QCD **ONLY** becomes clear in certain circumstances: in the heavy quark limit the soft QCD for quark-antiquark or quark-quark interactions can become much simpler.

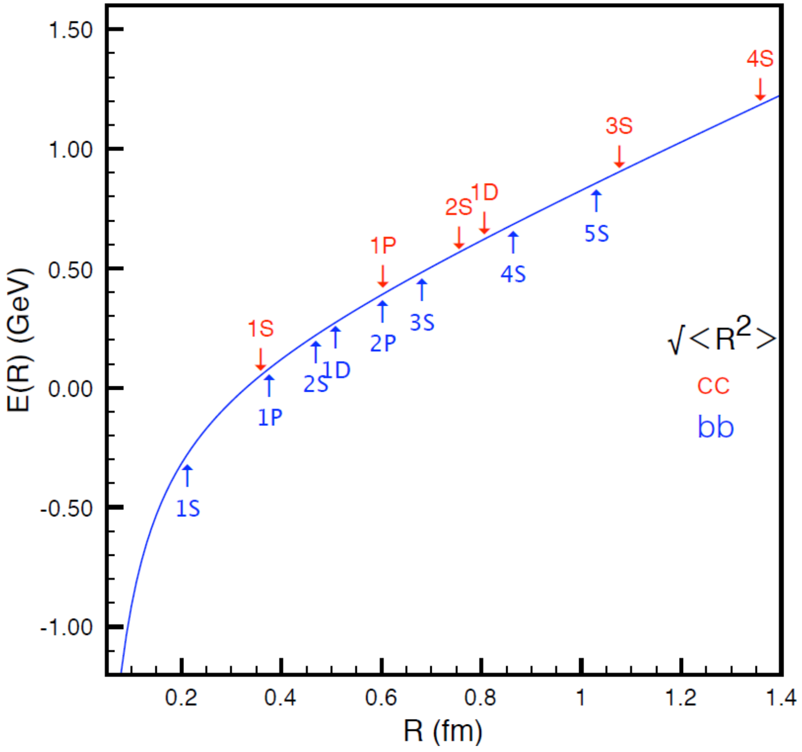

Quenched LQCD simulation

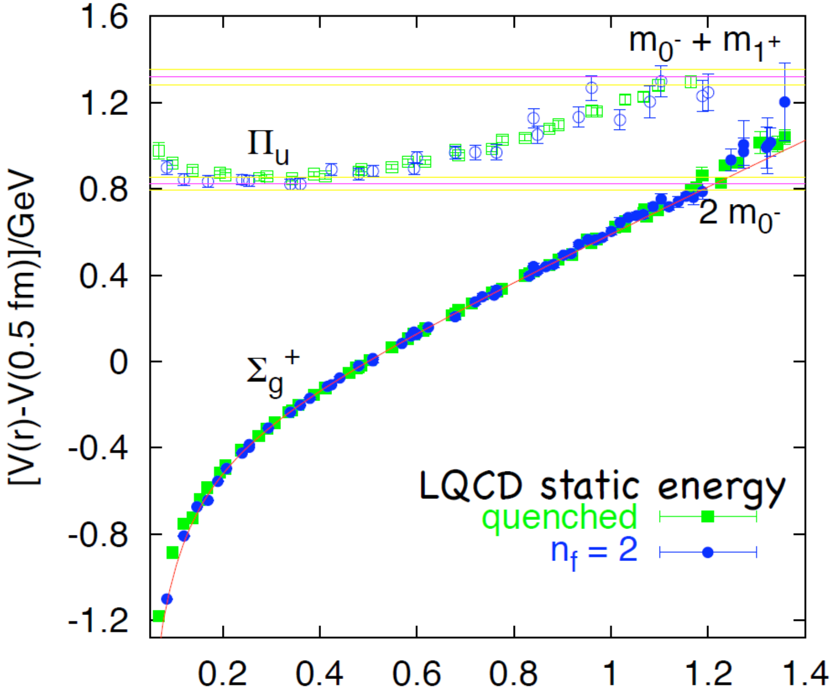

G. S. Bali, et al., Phys. Rev. D62, 054503 (2000)
M. Foster and C. Michael (UKQCD), Phys. Rev. D59, 094509 (1999)

The QM state $\chi_{c1}(2P)$ is about 60 MeV higher than the physical state $X(3872)$.

$n^{2S+1}L_J$	Name	J^{PC}	Exp. [6]	[8]	[11]	LP	SP
1^3S_1	J/ψ	1^{--}	3097[a]	3090	3097	3097	3097
1^1S_0	$\eta_c(1S)$	0^{-+}	2984[a]	2982	2979	2983	2984
2^3S_1	$\psi(2S)$	1^{--}	3686[a]	3672	3673	3679	3679
2^1S_0	$\eta_c(2S)$	0^{-+}	3639[a]	3630	3623	3635	3637
3^3S_1	$\psi(3S)$	1^{--}	4040[a]	4072	4022	4078	4030
3^1S_0	$\eta_c(3S)$	0^{-+}	...	4043	3991	4048	4004
4^3S_1	$\psi(4S)$	1^{--}	4415?	4406	4273	4412	4281
4^1S_0	$\eta_c(4S)$	0^{-+}	...	4384	4250	4388	4264
5^3S_1	$\psi(5S)$	1^{--}	...	...	4463	4711	4472
5^1S_0	$\eta_c(5S)$	0^{-+}	...	...	4446	4690	4459
1^3P_2	$\chi_{c2}(1P)$	2^{++}	3556[a]	3556	3554	3552	3553
1^3P_1	$\chi_{c1}(1P)$	1^{++}	3511[a]	3505	3510	3516	3521
1^3P_0	$\chi_{c0}(1P)$	0^{++}	3415[a]	3424	3433	3415	3415
1^1P_1	$h_c(1P)$	1^{+-}	3525[a]	3516	3519	3522	3526
2^3P_2	$\chi_{c2}(2P)$	2^{++}	3927[a]	3972	3937	3967	3937
2^3P_1	$\chi_{c1}(2P)$	1^{++}	...	3925	3901	3937	3914
2^3P_0	$\chi_{c0}(2P)$	0^{++}	3918?	3852	3842	3869	3848
2^1P_1	$h_c(2P)$	1^{+-}	...	3934	3908	3940	3916

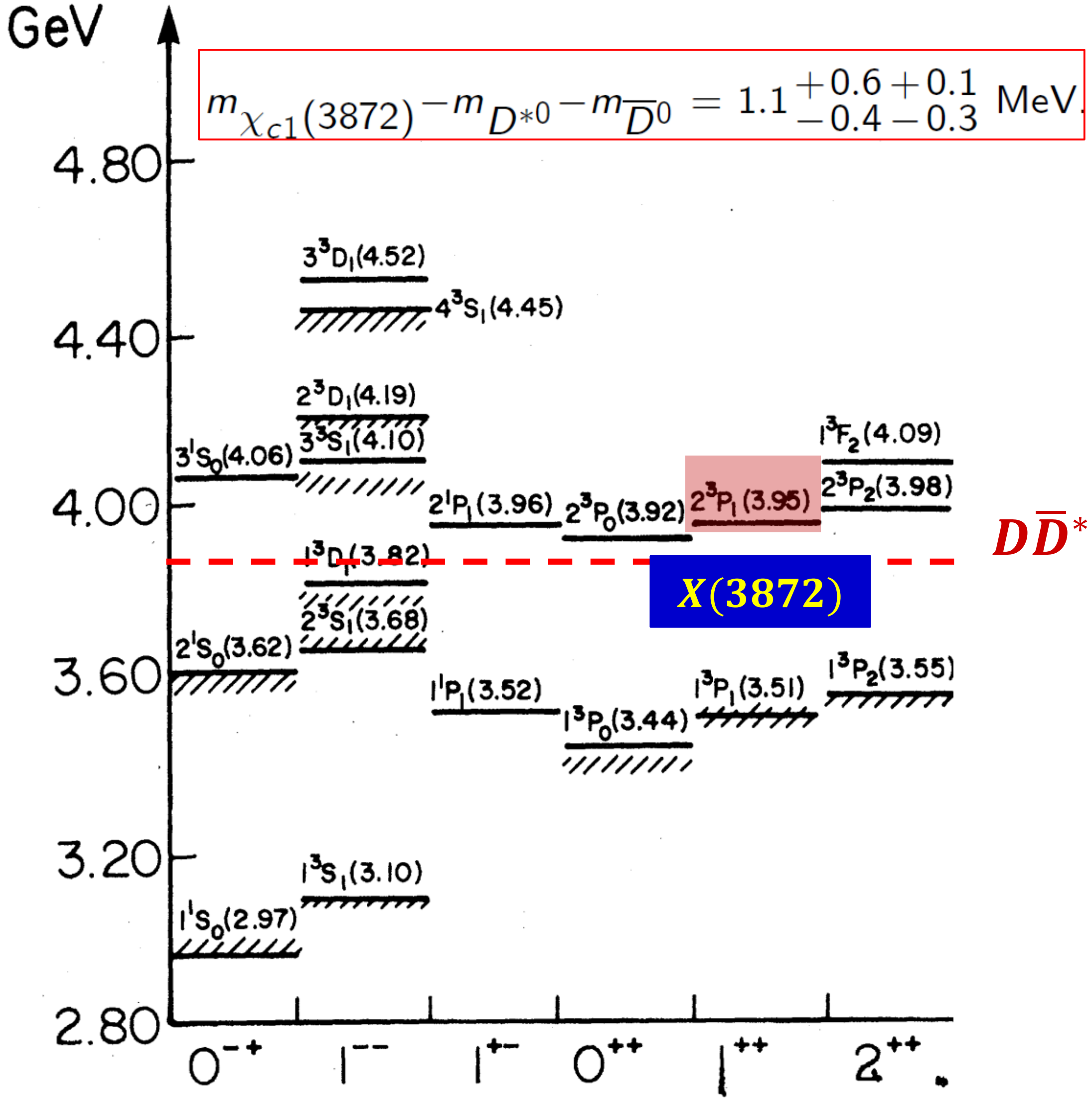

W.J. Deng et al., PRD95, 034026 (2017)

Godfrey and Isgur, PRD32, 189 (1985)

[8] T. Barnes, S. Godfrey, and E. S. Swanson, PRD 72, 054026 (2005).
[11] B. Q. Li and K. T. Chao, PRD 79, 094004 (2009).

Open threshold effects: A missing piece of dynamics in the potential QM

Quenched LQCD simulation

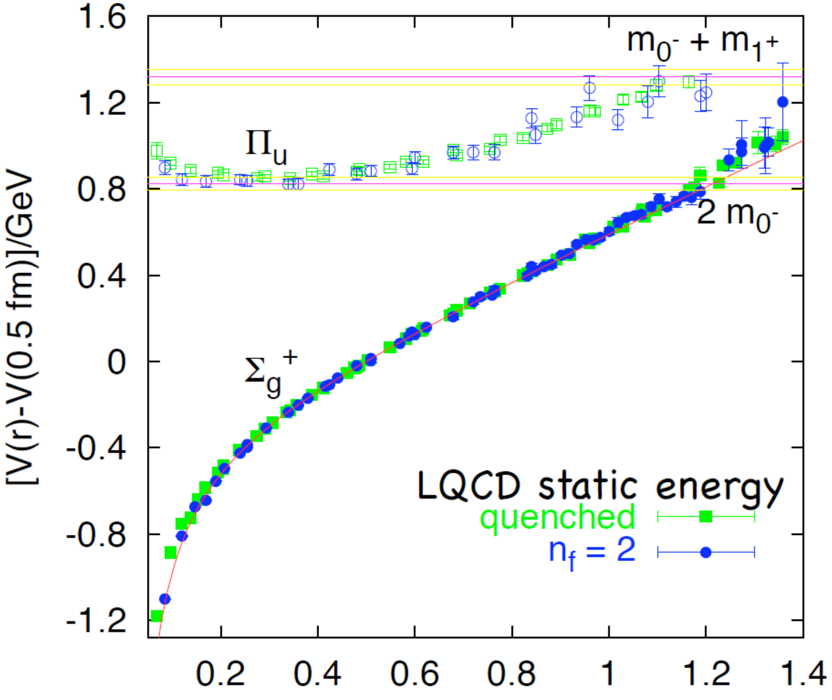

Unquenched LQCD simulation

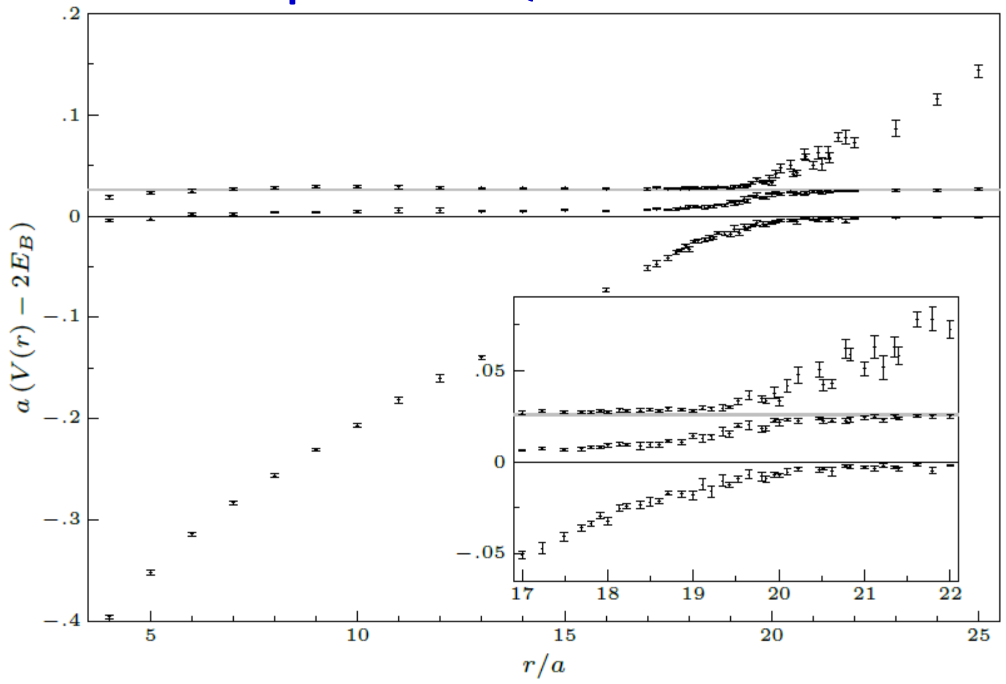

The creation energy for a quark pair with $J^{PC} = 0^{++}$: $E \simeq 2m_\pi \simeq 280$ MeV.

The radial excitation energy for nucleon: $m_{N(1440)} - m_{N(938)} \simeq 502$ MeV.

The orbital excitation energy for nucleon: $m_{N(1535)} - m_{N(938)} \simeq 597$ MeV.

However, the effects of the open channels on the soft QCD potential is also evident!

G. S. Bali, et al., Phys. Rev. D62, 054503 (2000)
M. Foster and C. Michael (UKQCD), Phys. Rev. D59, 094509 (1999)
J. Bulava, et al., Phys. Lett. B793, 493 (2019)

The narrow two-body open thresholds:

Impact on the spectrum should have some systematic features.

	$S-wave(L=0)$	$P-wave(L=1)$
PP	$0^{+(\pm)}$	$1^{-(\pm)}$
PV	$1^{+(\pm)}$	$0^{-(\pm)},\ 1^{-(\mp)},\ 2^{-(\pm)}$
VV	$0^{+(+)},\ 1^{+(-)},\ 2^{+(+)}$	$1^{-(+)};$ $0^{-(-)},\ 1^{-(-)},\ 2^{-(-)};$ $1^{-(+)},\ 2^{-(+)},\ 3^{-(+)}$
PA	$1^{-(-)}$	$\ldots\ldots$
VA	$0^{-(\pm)},\ 1^{-(\mp)},\ 2^{-(\pm)}$	$\ldots\ldots$

- The number of states would depend on the interactions between the threshold hadrons.
- So far, the S-wave phenomena is evident.
- Model-building is required.

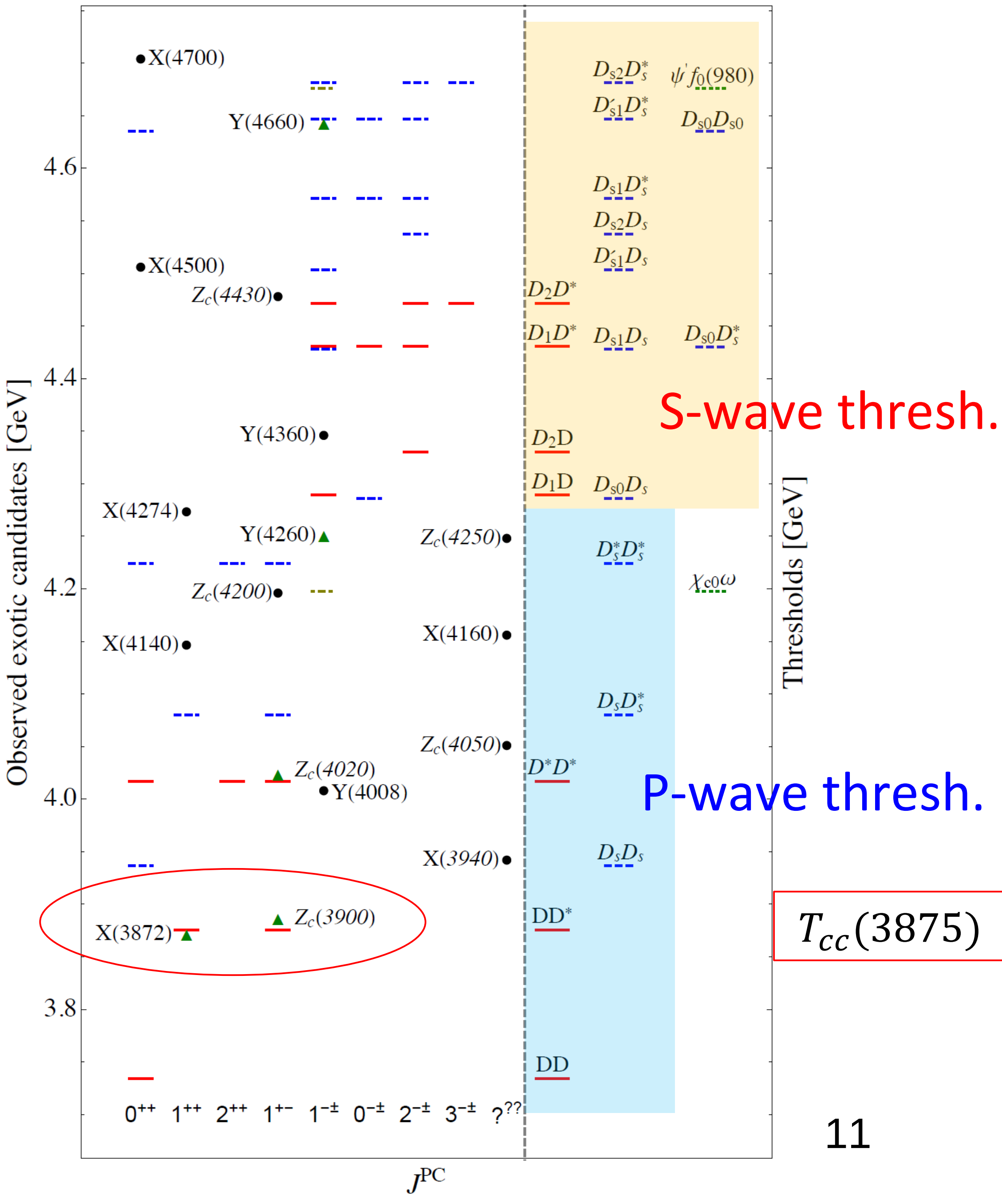

F.-K. Guo, C. Hanhart, U.-G. Meissner, Q. Wang, Q. Zhao, B.-S. Zou, Rev. Mod. Phys. 90, 015004 (2018)

Implementation of EFT with heavy quark symmetry (HQS) and heavy quark spin symmetry (HQSS)

X.-K. Dong, F.-K. Guo, B.-S. Zou, Progr. Phys. 41 (2021) 65 [arXiv:2101.01021]

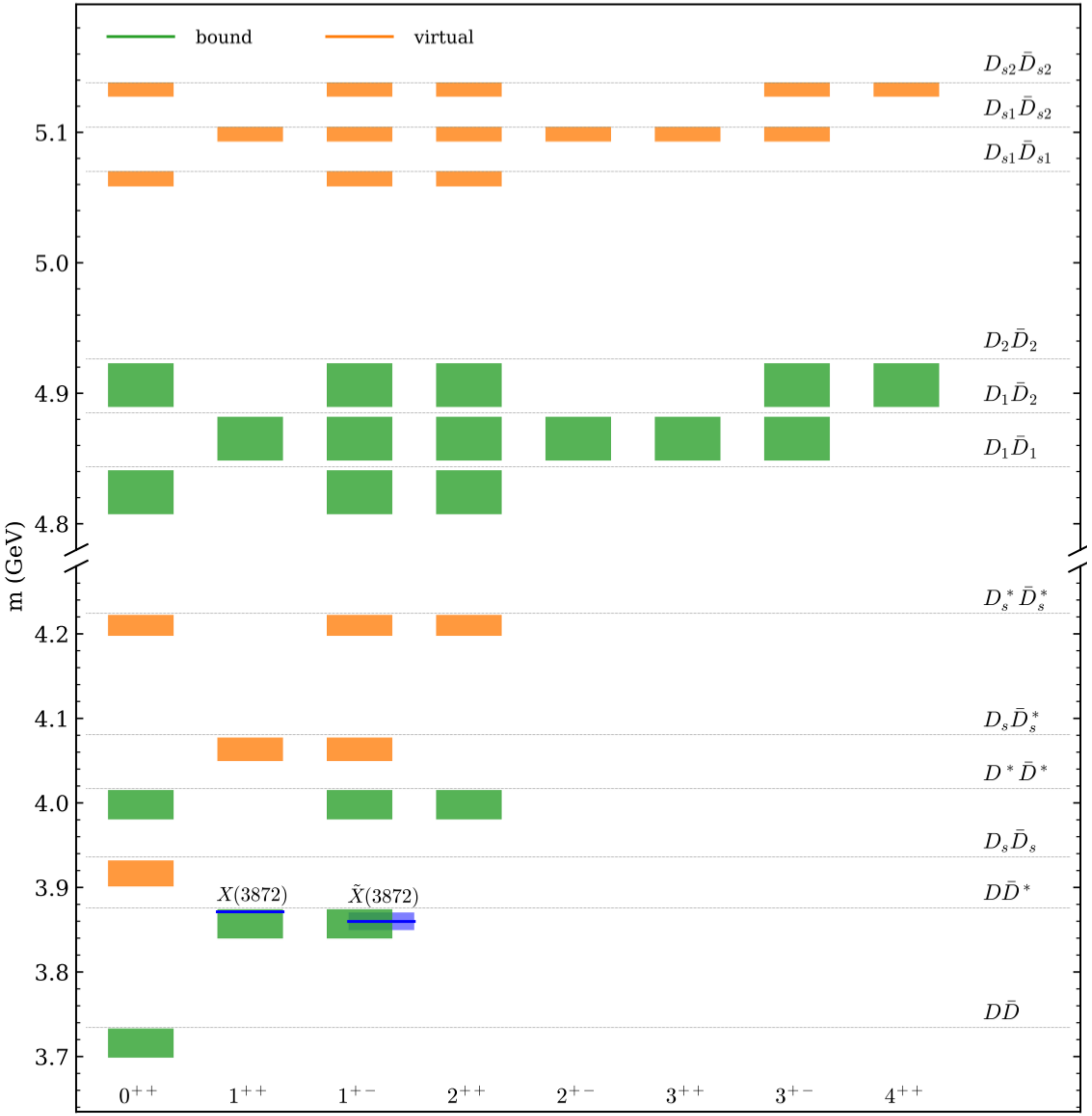

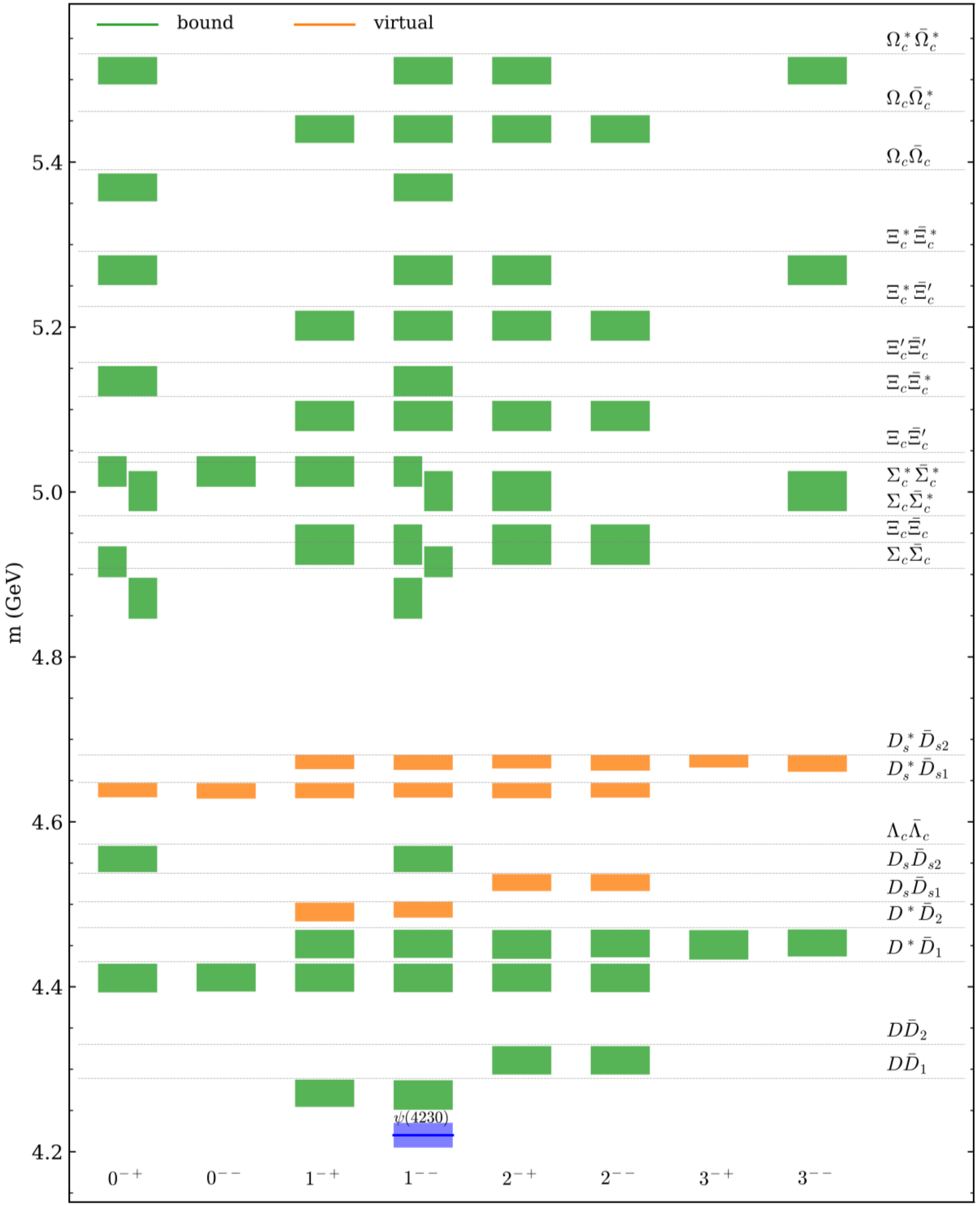

S wave thresholds and effects on the lineshapes

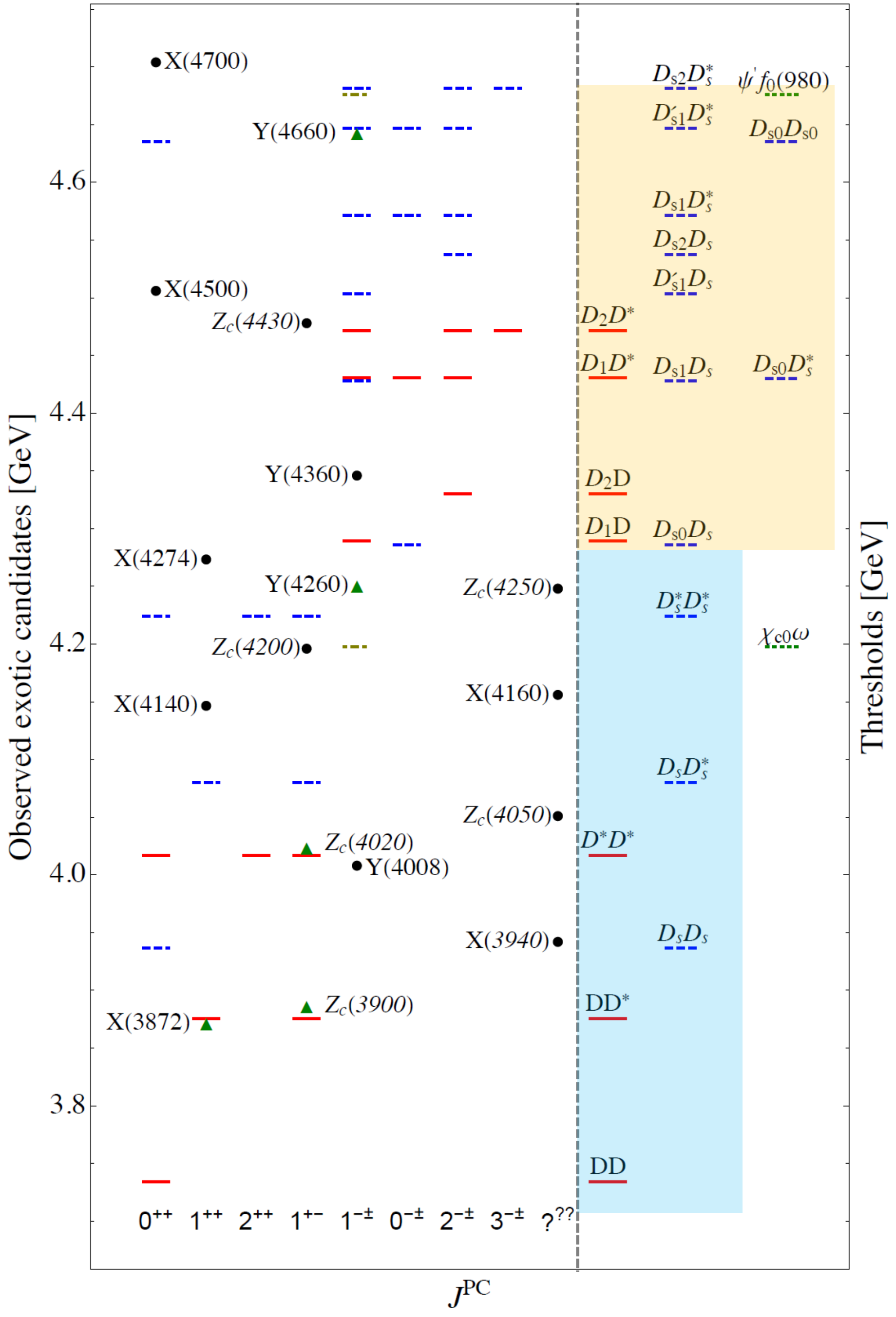

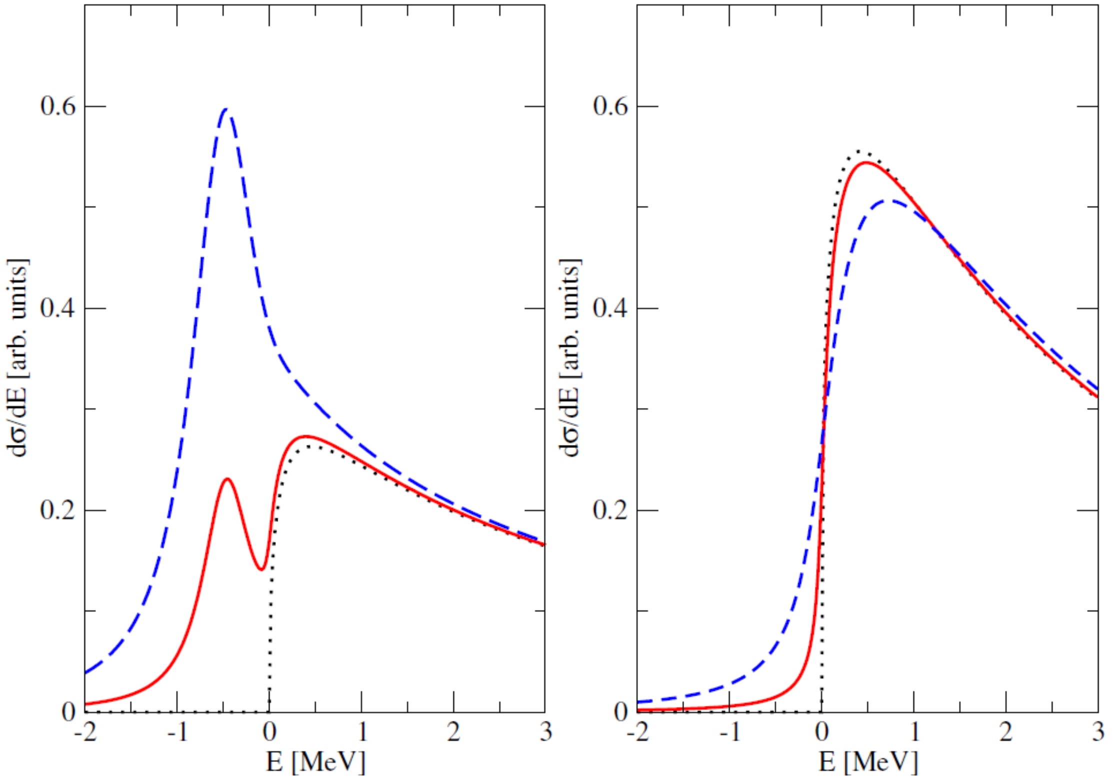

FIG. 10 Line shapes that emerge for a bound state (left panel) and for a virtual state (right panel) once one of the constituents is unstable. The dotted, solid and dashed line show the results for $\Gamma = 0, 0.1$ and 1 MeV, respectively. The other parameters of the calculation are given in Eq. (36).

F.-K. Guo, C. Hanhart, U.-G. Meissner, Q. Wang, Q. Zhao, B.-S. Zou, Rev. Mod. Phys. 90, 015004 (2018)

2. Vector charmonia probed in e^+e^- annihilations

---The property of the vector charmonium $Y(4260)$ in different scenarios

1) Observations of Y(4260)

First evidence from BaBar in $e^+e^- \rightarrow \gamma_{ISR}\, J/\psi\pi^+\pi^-$ and quickly confirmed by CLEO-c and Belle

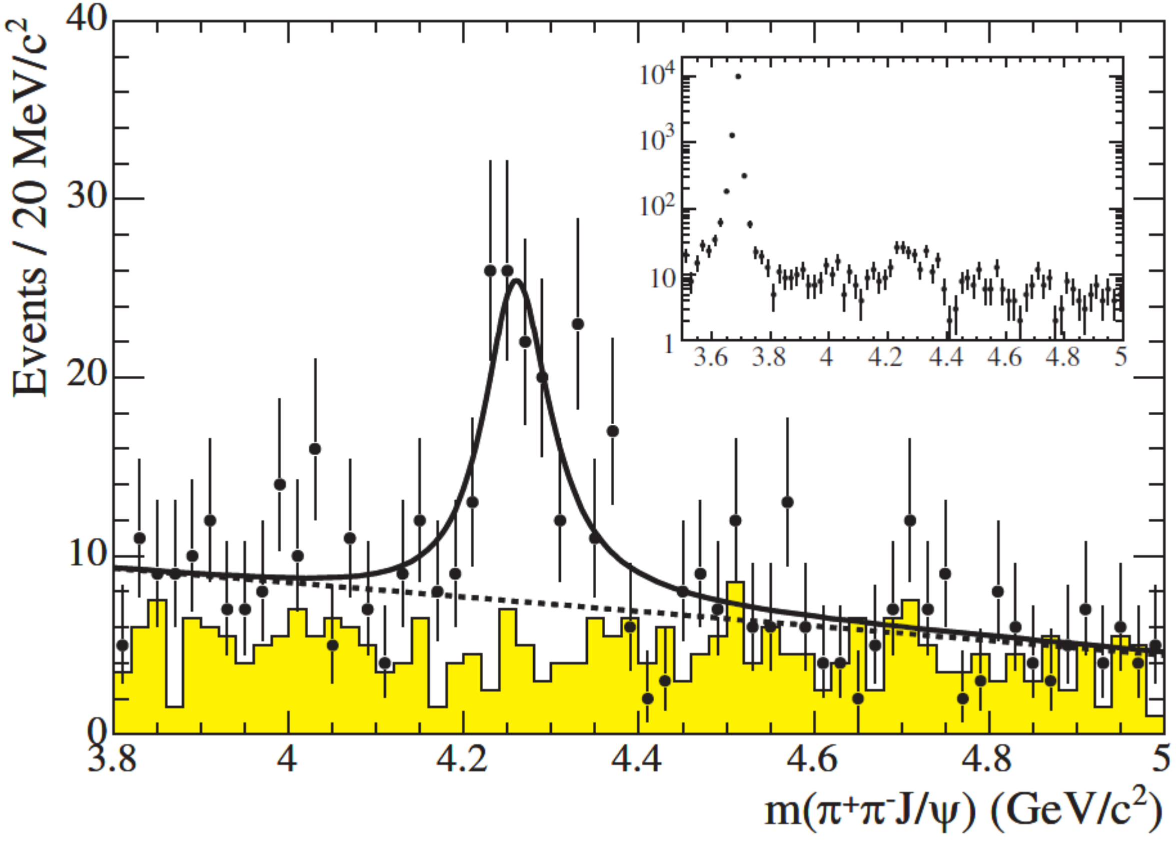

$$4259 \pm 8(\mathrm{stat})^{+2}_{-6}(\mathrm{syst})\ \mathrm{MeV}/c^2$$

$$88 \pm 23(\mathrm{stat})^{+6}_{-4}(\mathrm{syst})\ \mathrm{MeV}/c^2$$

BaBar, *Phys.Rev.Lett.* 95 (2005) 142001

* Particle Data Group renames $\boldsymbol{Y(4260)}$ as $\boldsymbol{\psi(4230)}$

One state or two states?

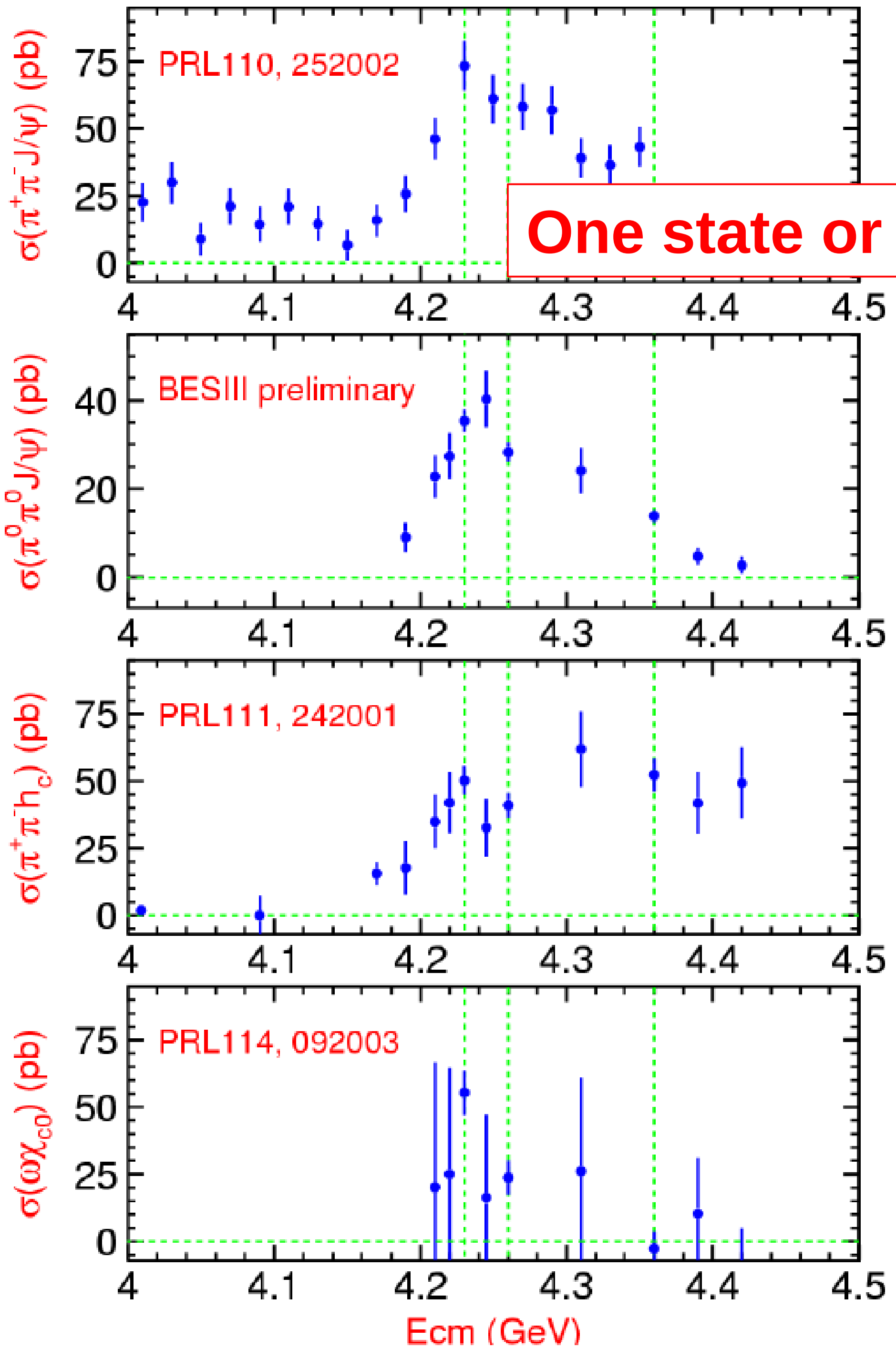

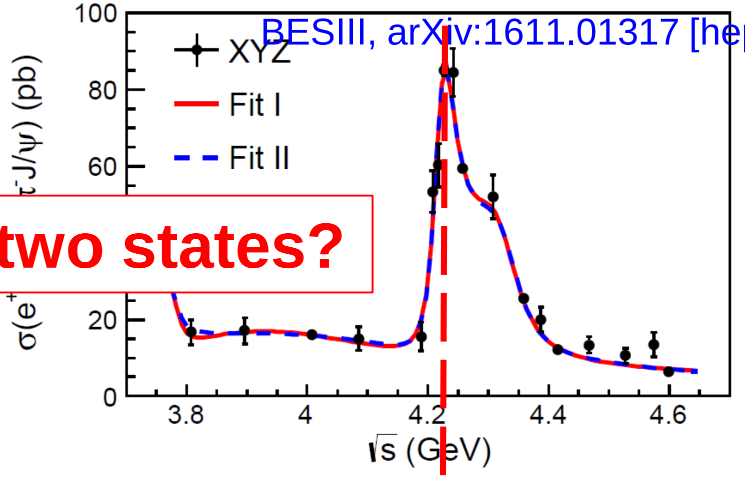

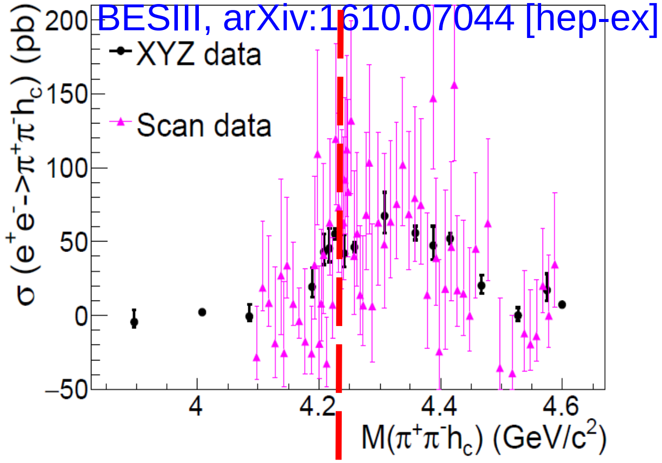

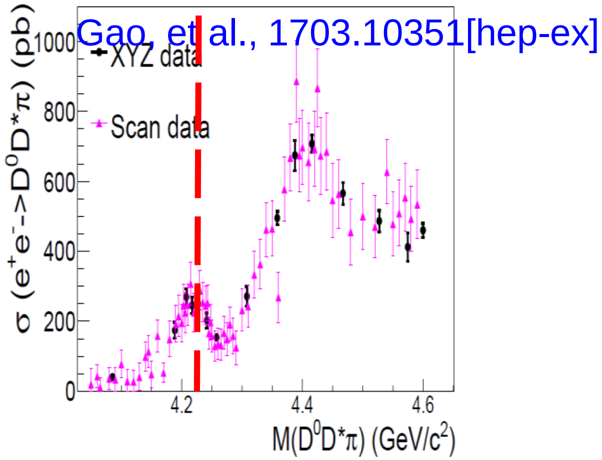

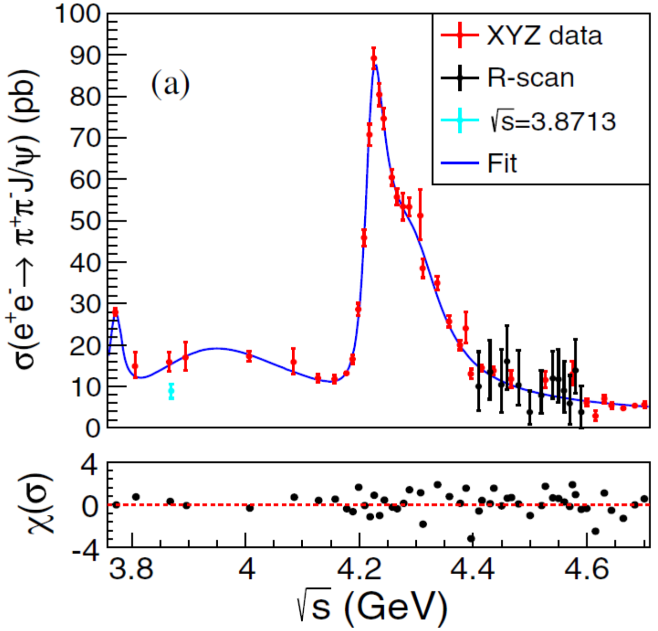

BESIII, PRD106, 072001 (2022)

Gao, et al., 1703.10351[hep-ex]

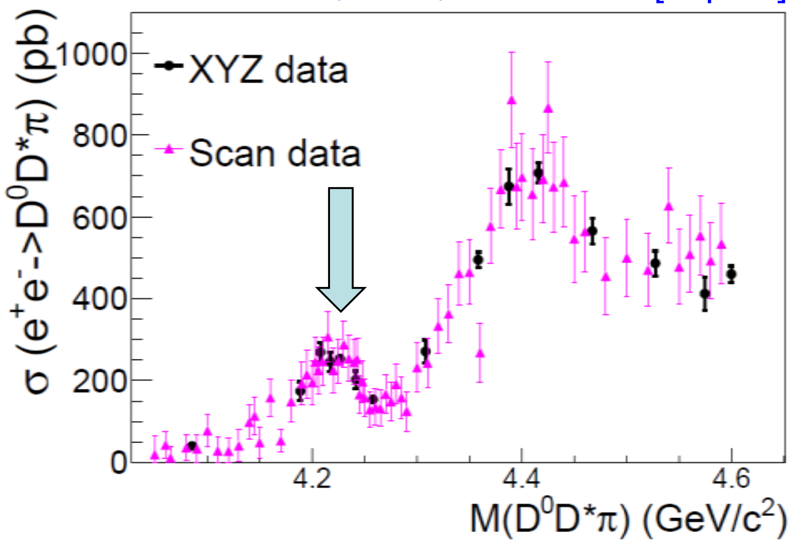

BESIII, 2112.06477[hep-ex]

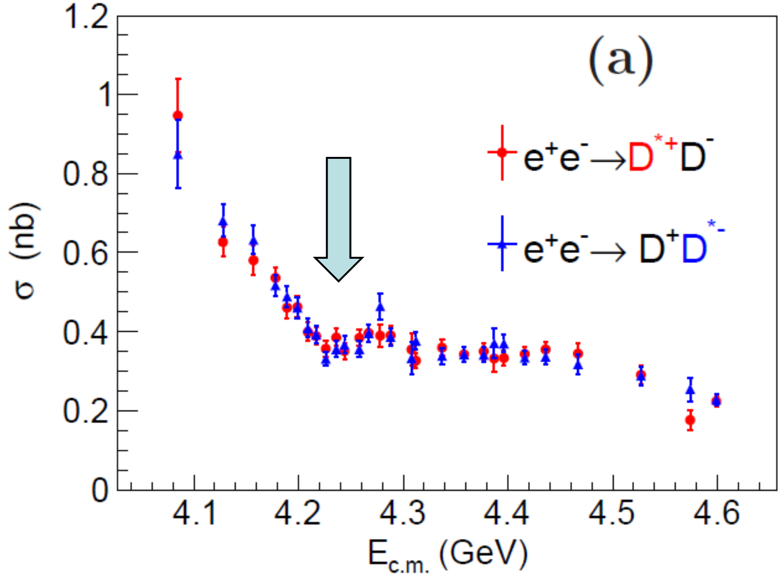

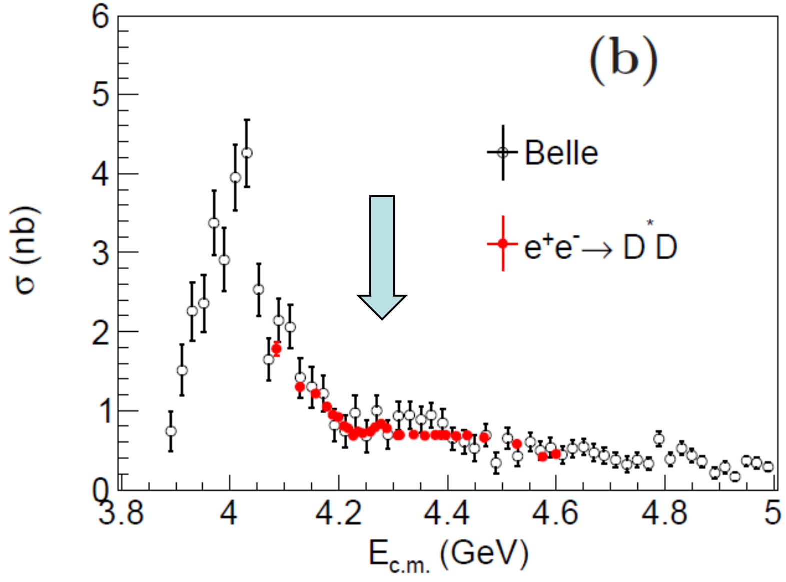

No apparent bump structure appears in the two-body open charm decays!

$\sigma(D^*\bar{D} + c.c.) \gg \sigma(D^*\bar{D}^*)$ at 4.23 GeV

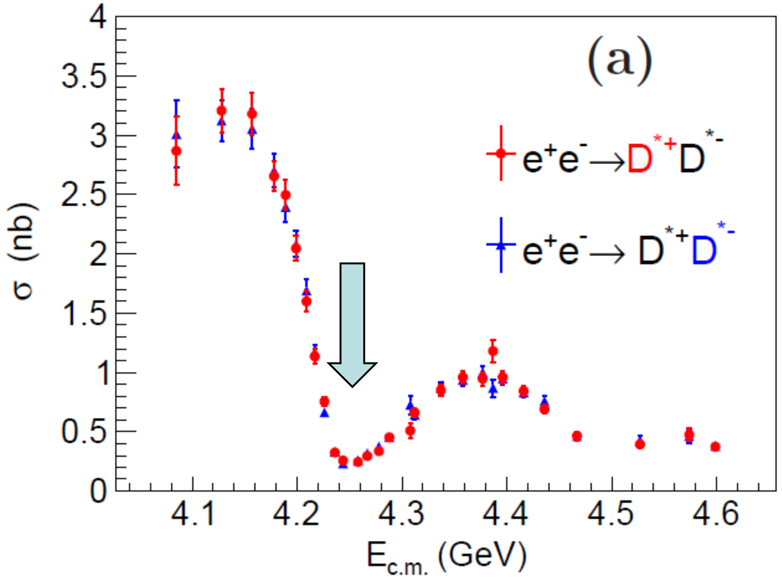

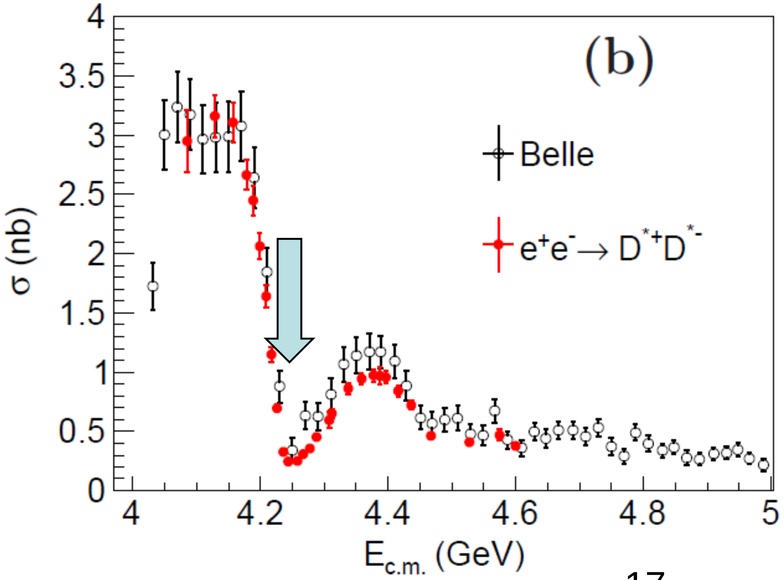

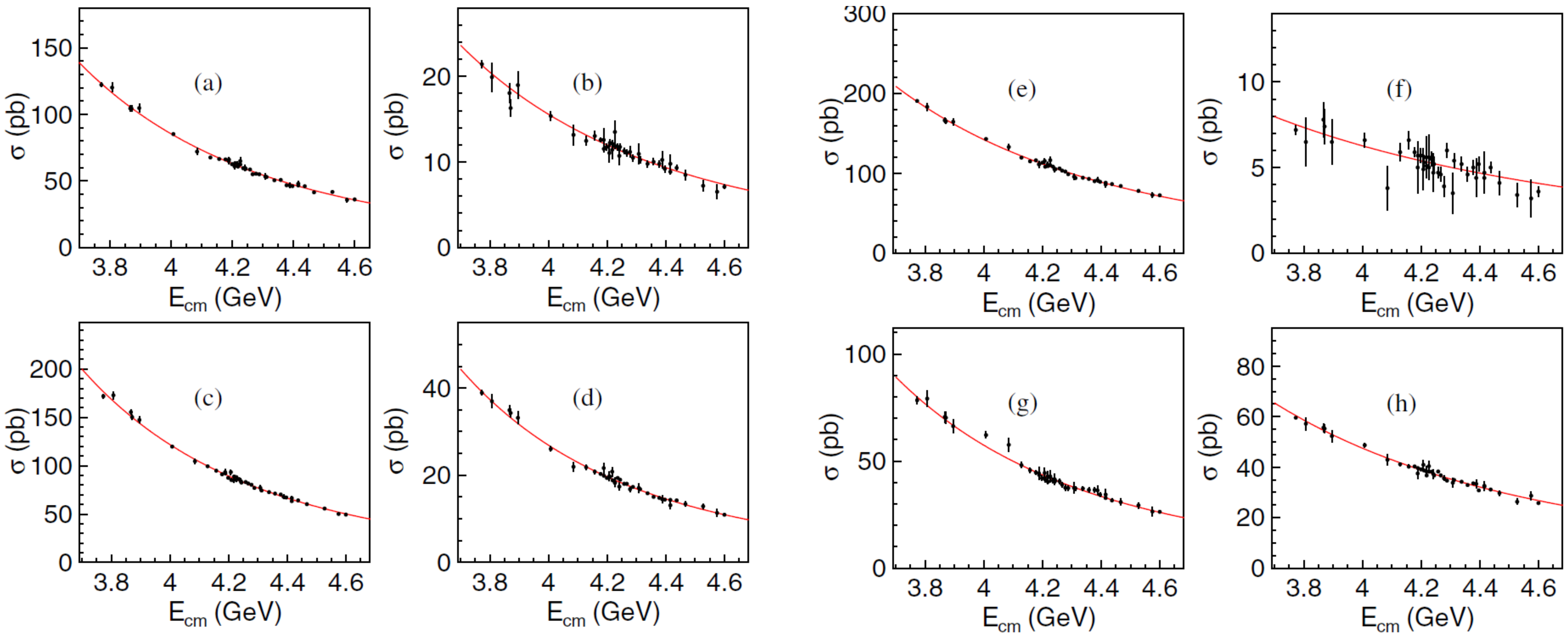

FIG. 3. Fits to dressed cross sections for (a) $e^+e^- \to K^+K^-\pi^+\pi^-$, (b) $e^+e^- \to K^+K^-K^+K^-$, (c) $e^+e^- \to \pi^+\pi^-\pi^+\pi^-$, (d) $e^+e^- \to p\bar{p}\pi^+\pi^-$, (e) $e^+e^- \to K^+K^-\pi^+\pi^-\pi^0$, (f) $e^+e^- \to K^+K^-K^+K^-\pi^0$, (g) $e^+e^- \to \pi^+\pi^-\pi^+\pi^-\pi^0$ and (h) $e^+e^- \to p\bar{p}\pi^+\pi^-\pi^0$ only considering contribution from continuum process. Points with error bars show the measured dressed cross sections. The red lines show the fit results.

No explicit experimental evidence for $Y(4260)$ is seen in the pure light-quark final states.

- *Phys.Rev.D* 104 (2021) 11, 112009; 2109.12751 [hep-ex]

Resonance parameters extracted around 4.26 GeV in different channels

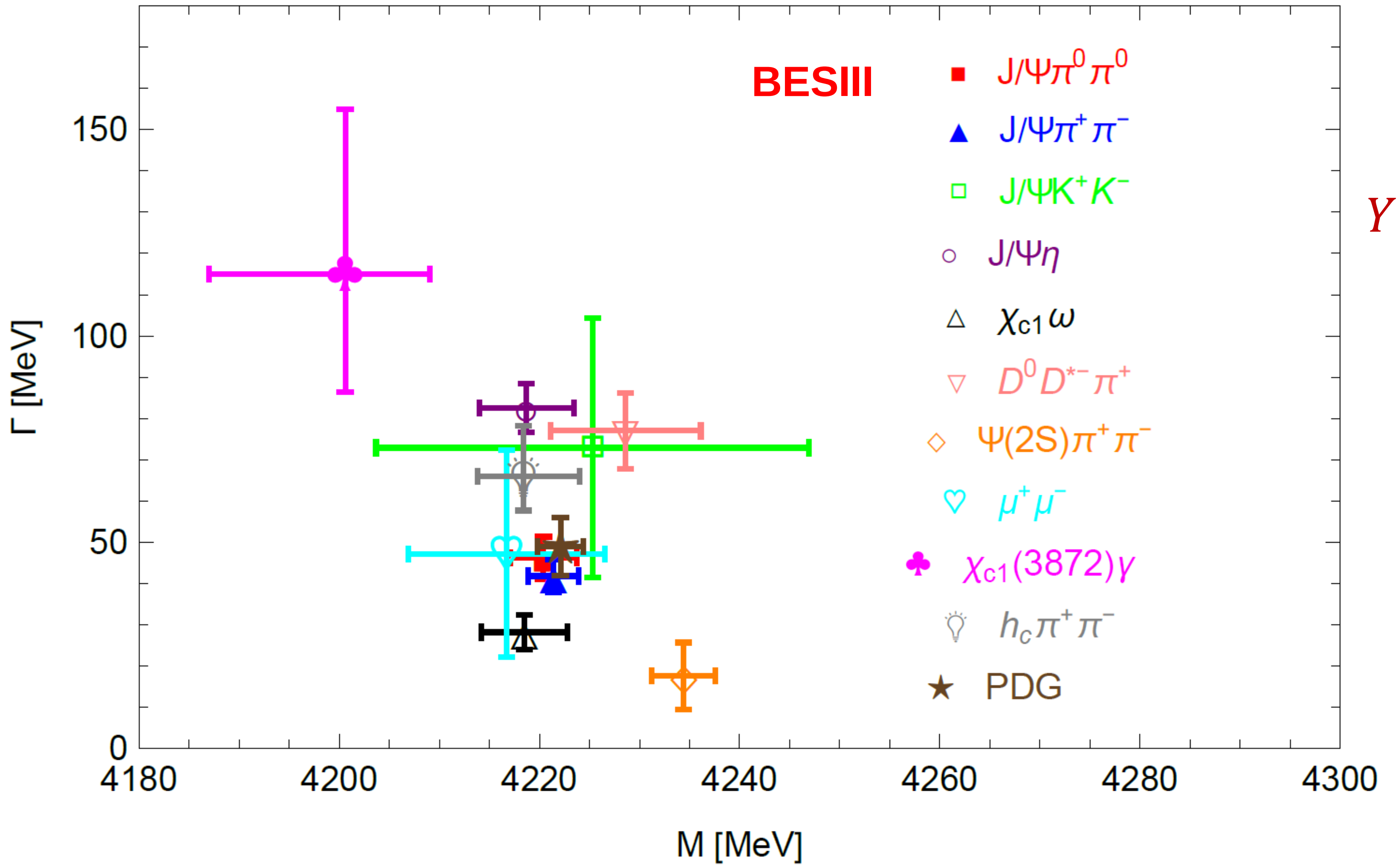

$Y(4260) \Rightarrow \psi(4230)$

A brief summary of the experimental status and a list of concerns:

1) Complicated structures in the vicinity of 4.22~4.26 GeV.
2) Relatively narrow structure for the lower peak if fitted by Breit-Wigner.
3) The pion angular distribution recoiling $Z_c(3900)$ in $Y(4260) \to \bar{D}D^*\pi$ indicates non-S-wave contributions.
4) The open-charm cross section seems to be larger than those for the hidden charm channel.
5) The signal of Y(4260) in $e^+e^- \to D^*\bar{D}^*$ needs to be clarified.
6) The lepton decay width will depend on how the total width is saturated.
7) The Breit-Wigner width may not be the pole width.
8) ……

Reac. channel	Total cross section (pb)
$\bar{D}D^*\pi + c.c.$	200~300
$J/\psi\pi^+\pi^-$	~80
$h_c\pi^+\pi^-$	~50
$\omega\chi_{c0}$	~50
$J/\psi\eta$	50~60
$J/\psi\eta'$	2~4
$\psi(2S)\pi^+\pi^-$	~20
$J/\psi K^+K^-$	~4
$\gamma\chi_{c1,2}$	4~5
$\pi^0Z_c^0(3900)$	6~7

2) Possible interpretations and reminder of some crucial issues

- ◆ **Tetraquark**
- ◆ **Hybrid**
- ◆ **Hadro-quarkonium**
- ◆ **Hadronic molecule**
- ◆ **Non-resonance structure**

- **Many papers on the properties of Y(4260), e.g. see recent reviews and reference therein:**
- H.-X. Chen, W. Chen, X. Liu and S.-L. Zhu, **Phys. Rept.** 639, 1 (2016)
- F.K. Guo, C. Hanhart, U.-G. Meissner, Q. Wang, Q. Zhao, B.-S. Zou, **Rev. Mod. Phys.** 90, 015004 (2018)
- A. Esposito, A. Pilloni and A.D. Polosa, **Phys. Rept.** 668, 1 (2017)
- Q. Wang and Q. Zhao, arXiv:2508.05304v1 [hep-ph], to appear in **Chinese Phys. Lett.**

• Predictions from the compact tetraquark scenario

The mass of a tetraquark is given by

$$M = M_{00} + B_c \frac{\boldsymbol{L}^2}{2} - 2a\boldsymbol{L}\cdot\boldsymbol{S} + 2\kappa_{cq}\left[(s_q \cdot s_c + (s_{\bar{q}} \cdot s_{\bar{c}}))\right]$$

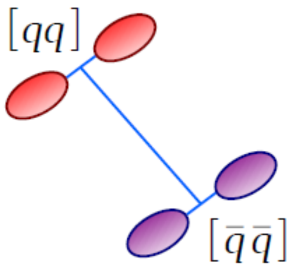

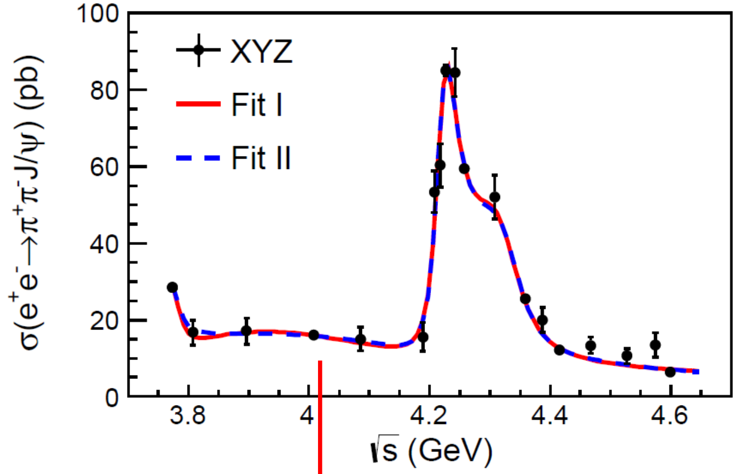

For a state with given ***J***, the mass can be estimated:

$$M = M_{00} + B_c \frac{L(L+1)}{2} + a[L(L+1) + S(S+1) - J(J+1)] + \kappa_{cq}\left[s(s+1) + \bar{s}(\bar{s}+1) - 3\right]$$

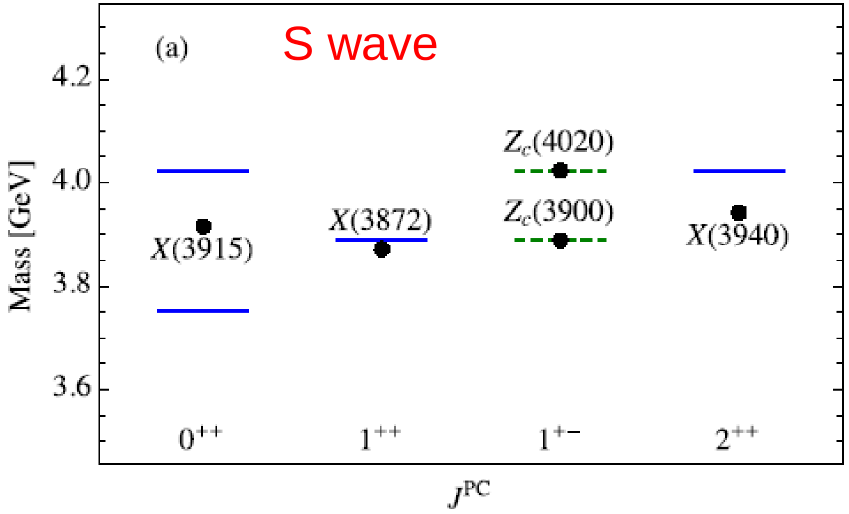

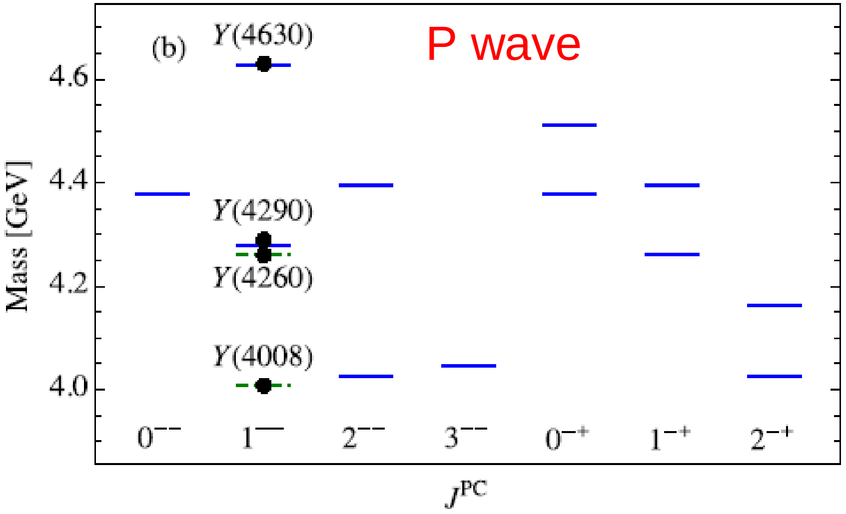

Y(4008) needs confirmation!

Extremely rich spectrum is predicted!

L. Maiani et al. **PRD 72**, 031502(R) (2005)
L. Maiani et al. **PRD 89**, 114010 (2014)
M. Cleven, F.- K. Guo, C. Hanhart, Q. Wang and Q. Zhao, **PRD 92**, 014005 (2015);
Q. Wang, **PRD 89**, 114013 (2014)

The updated P-wave tetraquark spectroscopy where the left panel is the spectroscopy with $\psi(4008)$ and $\psi(4230)$ as inputs, and the right one is the spectroscopy with $\psi(4230)$ and $\psi(4360)$ as inputs.

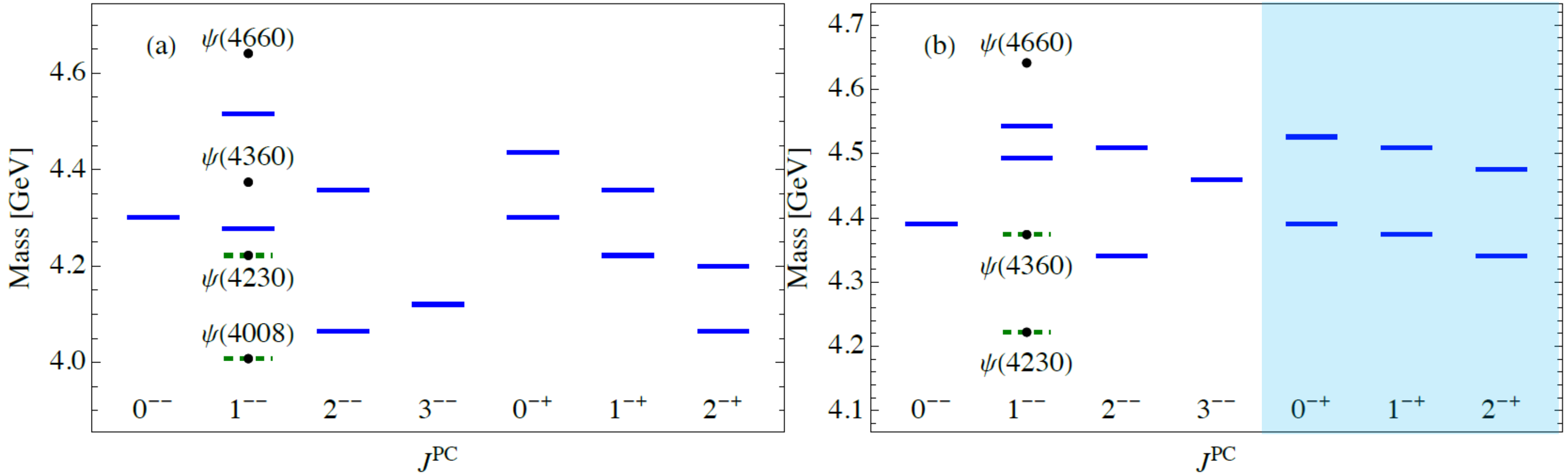

The P-wave diquark-antidiquark tetraquark supermultiplet with tensor force.

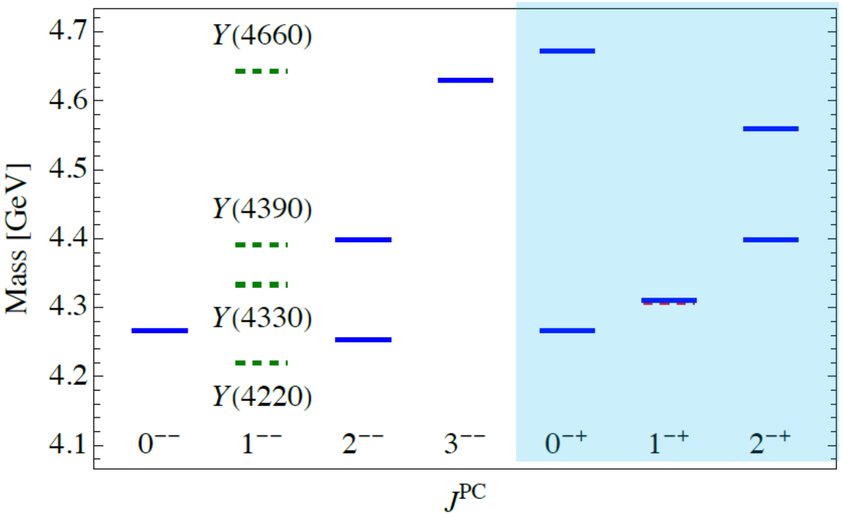

- Significant changes to the energy levels with the tensor force included.
- However, the description of the vector charmonium spectrum has not been improved.
- Access to exotic quantum numbers are allowed, e.g. 0^{--} and 1^{-+}.

• Predictions from the hybrid scenario

- Lowest gluon fields generate adiabatic potential on which the quark motion can be described.
- The flux tube may be excited on which the quark motion in the adiabatic potential of such excited gluon field configurations will give access to **hybrid states**.
- The decays of both conventional and exotic hadrons can be well described by the flux tube breaking mechanism.

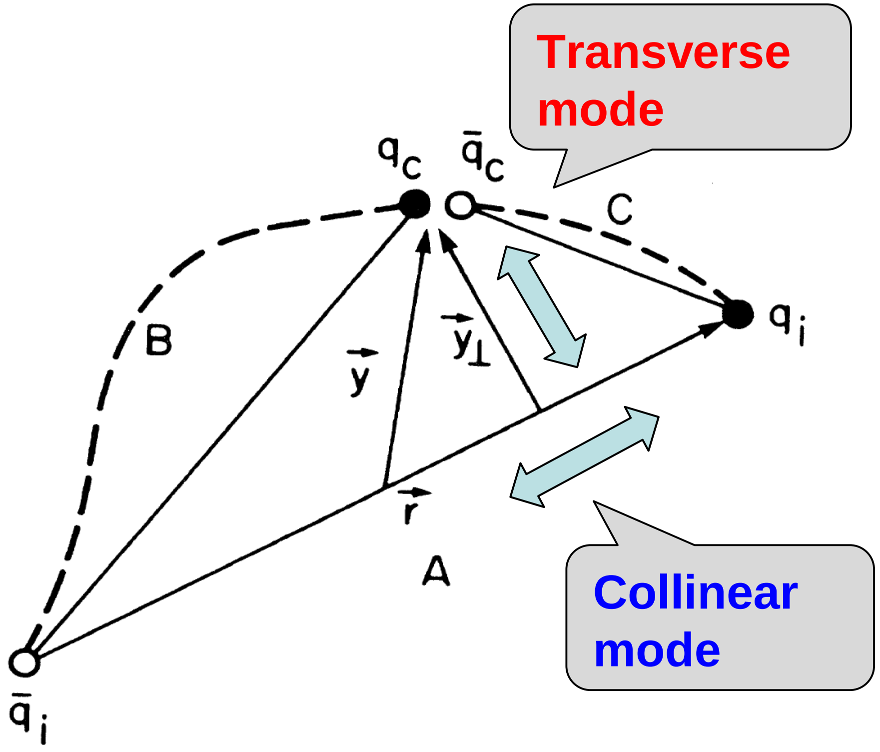

Flux tube model Hamiltonian:

$$H = H_{\text{quarks}} + H_{\text{flux tube}},$$

$$H_{\text{quarks}} = -\frac{1}{2m_q}\vec{\nabla}_q^2 - \frac{1}{2m_{\bar{q}}}\vec{\nabla}_{\bar{q}}^2 + V_{q\bar{q}},$$

$$H_{\text{fluxtube}} = b_0 R + \sum_n \left[\frac{p_n^2}{2b_0 a} + \frac{b_0}{2a}(y_n - y_{n+1})^2\right]$$

N. Isgur and J. Paton, PLB124 (1983) 247-251; PRL54 (1985) 869; PRD31 (1985) 2910

Lowest hybrid in the flux-tube model

Collinear mode

Transverse mode

$J_q^{P(C)} = 1^{-(-)}$

$\boldsymbol{J}_g = \boldsymbol{S}_g + \boldsymbol{L}_g,$

$J_g^{PC} = 1^{+-}$

$$J^{P(C)} = (0, 1, 2)^{-(+)}$$

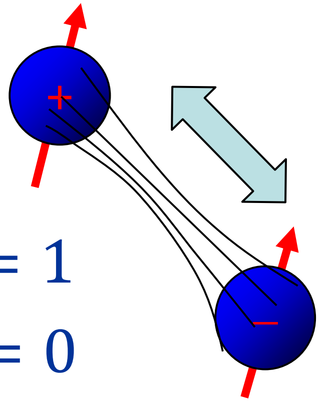

$S_q = 1$

$L_q = 0$

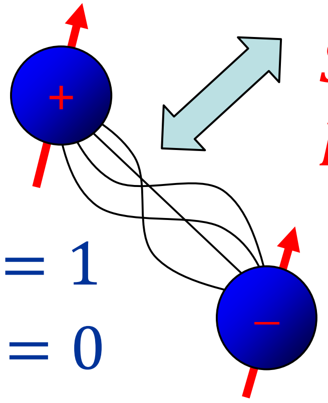

$S_g = 1$

$L_g > 0$

$S_q = 1$

$L_q = 0$

$J_q^{P(C)} = 0^{-(+)}$

$\boldsymbol{J}_g = \boldsymbol{S}_g + \boldsymbol{L}_g,$

$J_g^{PC} = 1^{+-}$

$$J^{P(C)} = 1^{--}$$

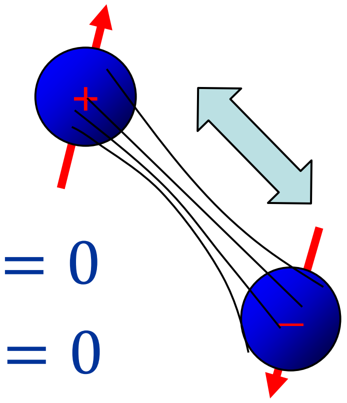

$S_q = 0$

$L_q = 0$

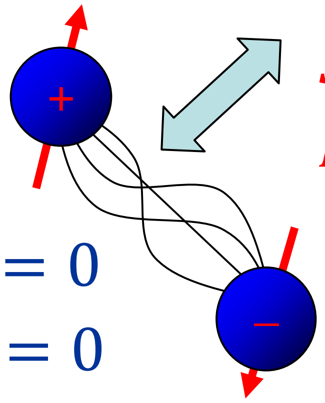

$S_g = 1$

$L_g > 0$

$S_q = 0$

$L_q = 0$

N. Isgur and J. Paton, PLB124 (1983) 247-251; PRL54 (1985) 869; PRD31 (1985) 2910

• Predictions from the hybrid scenario

1. In the hybrid picture the di-lepton coupling of $\psi(4230)$ is highly suppressed.
2. As the ground state vector charmonium hybrid, its decays into a pair of ground-state S-wave charmed mesons of the same spatial size will be suppressed (Broken down due to HQS breaking?)
3. The relative partial decay rates of $\psi(4230)$ to the S-wave open charmed pair is predicted to be $\Gamma(\psi(4230) \to D\,\bar{D}) : \Gamma(\psi(4230) \to D^*\,\bar{D} + c.c.) : \Gamma(\psi(4230) \to D^*\,\bar{D}^*) = 1 : 0 : 3$, where $\psi(4230) \to D^*\,\bar{D} + c.c.$ is forbidden (Seem to be contradicting with the exp. observation: $\sigma(D^*\bar{D} + c.c.) \gg \sigma(D^*\bar{D}^*)$ at 4.23 GeV).
4. ……

- S. L. Zhu, Phys. Lett. B 625, 212 (2005) [arXiv:hep-ph/0507025 [hep-ph]].
- F. E. Close and P. R. Page, Phys. Lett. B 628, 215-222 (2005) [arXiv:hep-ph/0507199 [hep-ph]].
- E. Kou and O. Pene, Phys. Lett. B 631, 164-169 (2005) [arXiv:hep-ph/0507119 [hep-ph]].
- E. Braaten and R. Bruschini, Phys. Rev. D 109, no.9, 094051 (2024)

• Predictions from the hadronic molecule scenario

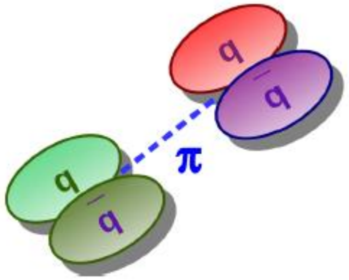

- **Hadronic molecule made of $\bar{D}D_1(2420) + c.c.$ with coupled channel effects.**

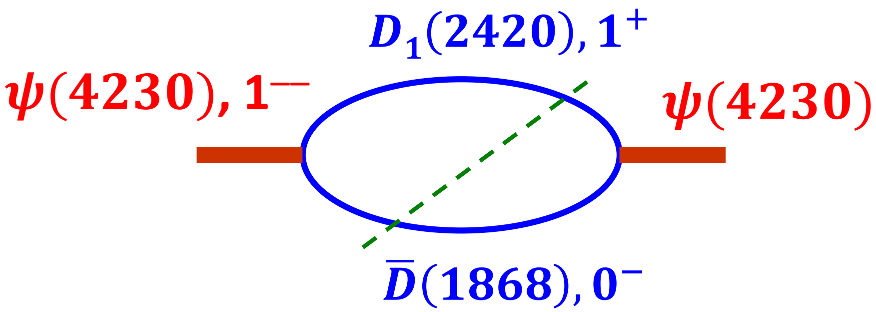

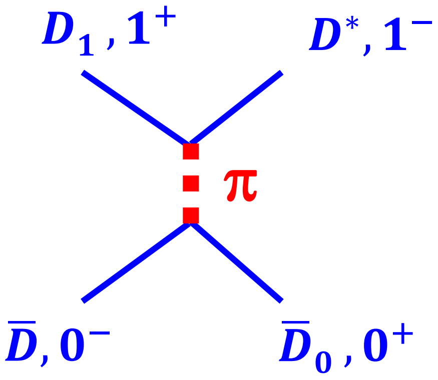

Depending on the binding mechanism, the isoscalar and isovector may not bind simultaneously:

$$\langle I, I_3 | \vec{\tau}_{(1)} \cdot \vec{\tau}_{(2)} | I, I_3 \rangle = 2\left[I(I+1) - 3/2\right] = \begin{cases} -3 & I = 0 \\ 1 & I = 1 \end{cases}$$

Q. Wang, C. Hanhart, QZ, PRL111, 132003 (2013)
Q. Wang et al., PRD89, 034001 (2014); M. Cleven et al., PRD90, 074039 (2014);
W. Qin, S.R. Xue, QZ, PRD94, 054035 (2016)

- **Correlations between Y(4260) and Zc(3900)/X(3872)**

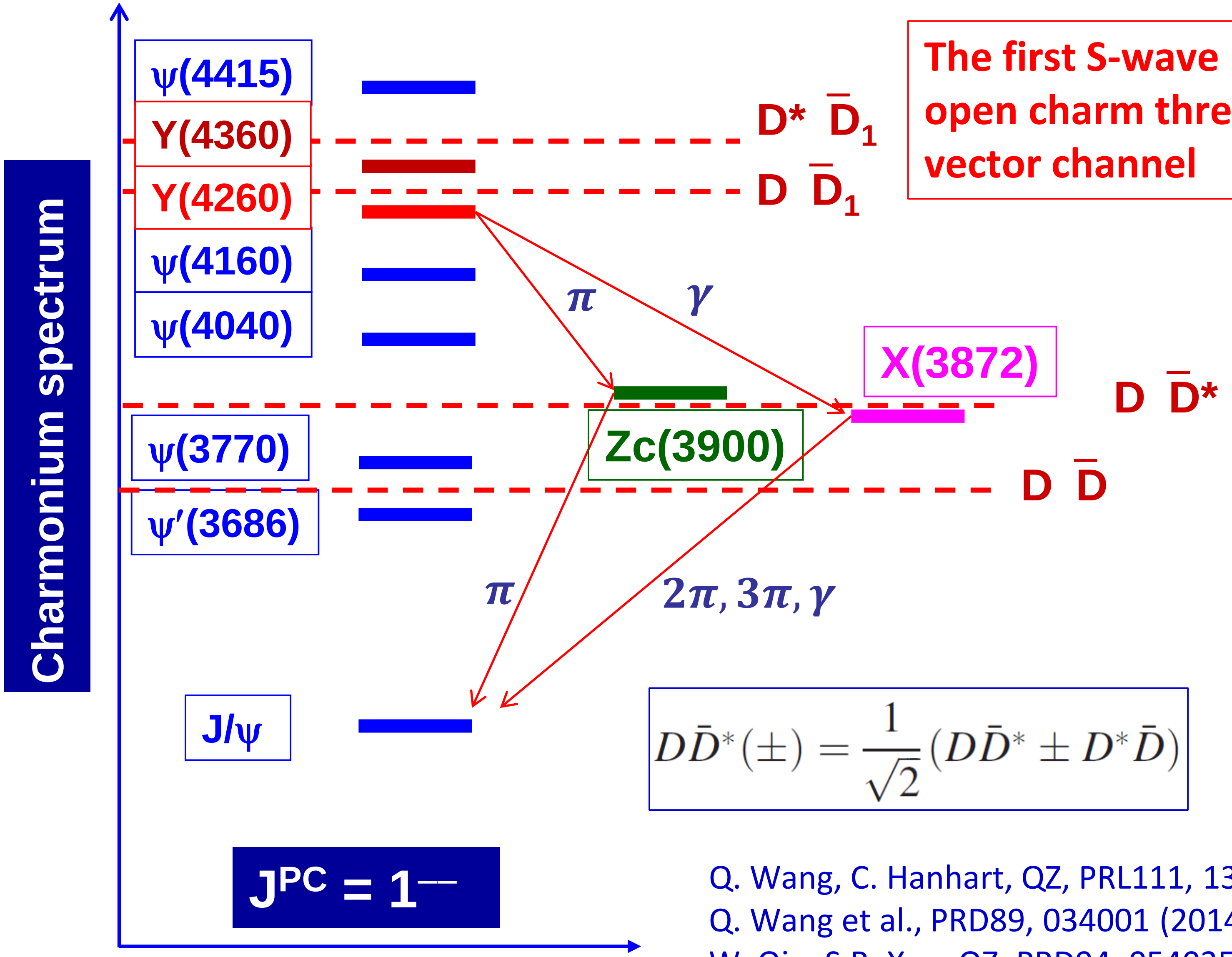

The first S-wave narrow open charm threshold in vector channel

$$D\bar{D}^*(\pm) = \frac{1}{\sqrt{2}}(D\bar{D}^* \pm D^*\bar{D})$$

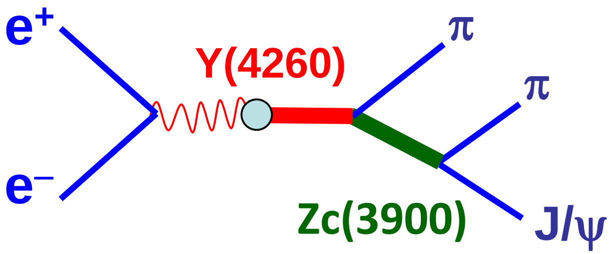

- **The production of Zc(3900) is strongly correlated with Y(4260) and enhanced by the triangle singularity kinematics.**

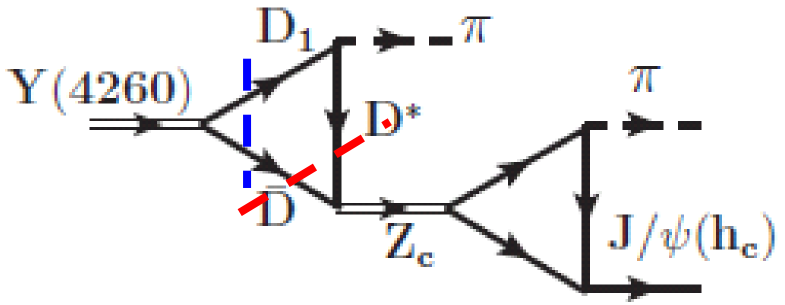

Q. Wang, C. Hanhart, QZ, PRL111, 132003 (2013); PLB(2013)
Q. Wang et al., PRD89, 034001 (2014); M. Cleven et al., PRD90, 074039 (2014);
W. Qin, S.R. Xue, QZ, PRD94, 054035 (2016)
L. von Detten, V. Baru, C. Hanhart, Q. Wang, D. Winney and QZ., PRD 109, 116002 (2024)

• Partners based on the heavy quark spin symmetry (HQSS)

- (D,D*) + (D,D*)

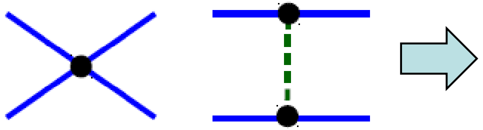

$J^{PC} = 0^{++}, 1^{++}, 1^{+-}, 2^{++}$

- (D_1,D_2) + (D,D*)

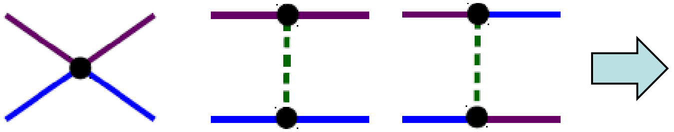

$J^{PC} = 1^{--}, 1^{-+}$

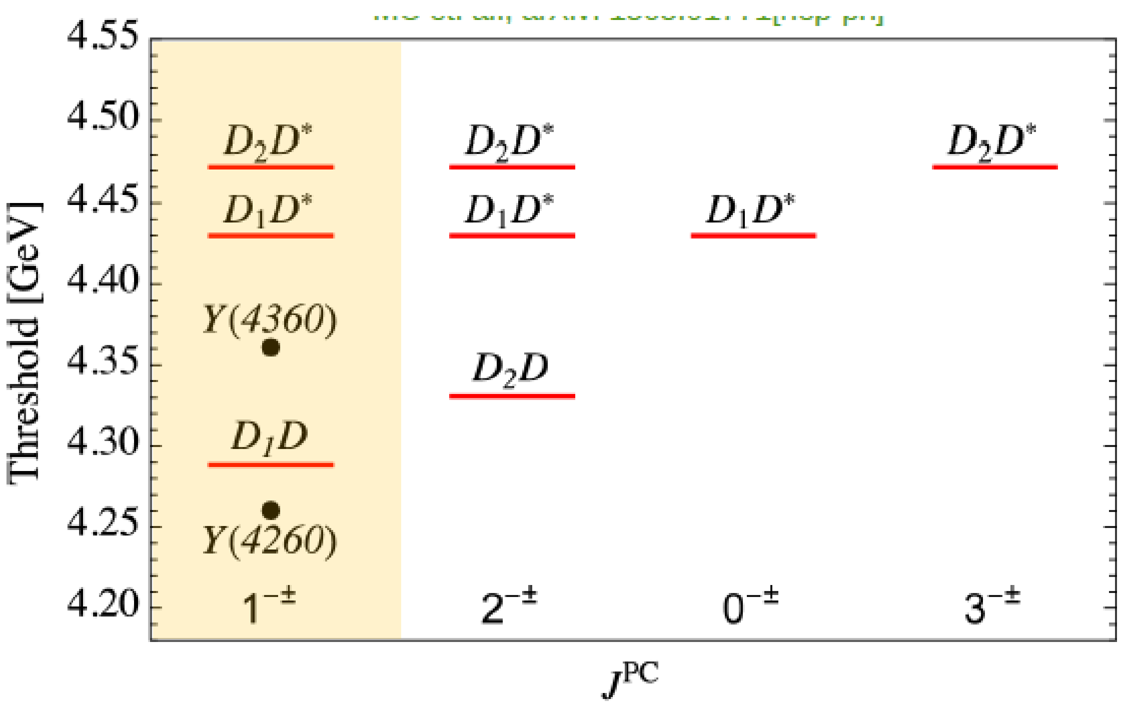

Experimental search for the 1^{-+} state in $e^+e^- \to \gamma\,\tilde{\psi}(1^{-+}) \to \gamma\bar{D}D^*\pi$ could be interesting.

Q. Wang, Phys. Rev. D 89, no.11, 114013 (2014) [arXiv:1403.2243 [hep-ph]].
X. K. Dong, Y. H. Lin and B. S. Zou, Phys. Rev. D 101, no.7, 076003 (2020) [arXiv:1910.14455 [hep-ph]].
X. Y. Zhang, P. P. Shi and F. K. Guo, Phys. Lett. B 867, 139603 (2025) [arXiv:2503.06259 [hep-ph]].

3. Non-perturbative mechanism probed in heavy hadron hadronic weak decays

Y. Cao, Y. Cheng and Q. Zhao, PRD 109, 073002 (2024)

Polarization puzzles with $D^0 \to \phi\rho^0$ and $\phi\omega$

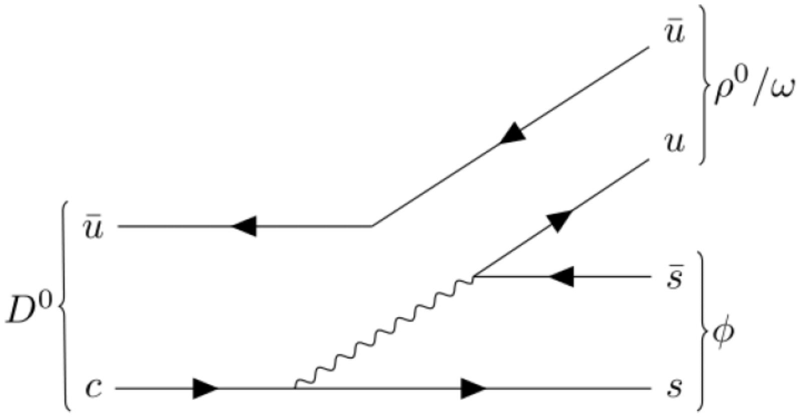

At the leading order, one would expect $Br(D^0 \to \phi\rho^0) \simeq Br(D^0 \to \phi\omega)$

$$u\bar{u} = \frac{1}{2}(u\bar{u} + d\bar{d}) + \frac{1}{2}(u\bar{u} - d\bar{d}) = \frac{1}{\sqrt{2}}(\omega + \rho^0)$$

However, significant differences arise from the experimental measurements:

(I) Negligibly small longitudinal polarization with the $\phi\omega$ channel:

$$f_L = 0.00 \pm 0.10 \pm 0.08$$

which corresponds to $f_L < 0.24$ at 95% C.L.

(II) Dominance of the S-wave in $D^0 \to \phi\rho^0$ suggests relatively large longitudinal pola. fraction f_L.

(III) Difference in b.r.s:

$$Br^{exp}(D^0 \to \phi\rho^0) = (1.56 \pm 0.13) \times 10^{-3}$$

$$Br^{exp}(D^0 \to \phi\omega) \simeq (0.65 \pm 0.10) \times 10^{-3}$$

There must be mechanisms beyond the leading tree-level transitions!

in unit of $(\times 10^{-3})$

$\phi\rho^0$	**S**	1.40 ± 0.12[21]
	P	0.08 ± 0.04[21]
	D	0.08 ± 0.03[21]
	T	-
	L	-
	Total	1.56 ± 0.13[21]
$\phi\omega$	T	0.65 ± 0.10[20]
	L	~ 0 [20]
	Total	0.65 ± 0.10[20]

[20] M. Ablikim et al., BESIII Colla., Phys. Rev. Lett., 128, 011803 (2022)

[21] P. d'Argent et al., JHEP, 05:143 (2017)

Parametrizing the short-distance transition mechanisms

- **Cabibbo-favored (CF) decays $(\sim V_{cs}V_{ud})$ via color suppressed transitions:**

Γ_{75}	$\overline{K}^*(892)^0\rho^0$, $\overline{K}^{*0} \to K^-\pi^+$	(1.01 ± 0.05) %
Γ_{76}	$\overline{K}^*(892)^0\rho^0$ transverse, $\overline{K}^{*0} \to K^-\pi^+$	(1.2 ± 0.4) %
Γ_{90}	$\overline{K}^*(892)^0\omega$, $\overline{K}^{*0} \to K^-\pi^+$, $\omega \to \pi^+\pi^-\pi^0$	$(6.5 \pm 3.0) \times 10^{-3}$
Γ_{114}	$\overline{K}^*(892)^0\omega$	(1.1 ± 0.5) %

$$u\bar{u} = \frac{1}{2}(u\bar{u} + d\bar{d}) + \frac{1}{2}(u\bar{u} - d\bar{d}) = \frac{1}{\sqrt{2}}(\omega + \rho^0)$$

$$d\bar{d} = \frac{1}{2}(u\bar{u} + d\bar{d}) - \frac{1}{2}(u\bar{u} - d\bar{d}) = \frac{1}{\sqrt{2}}(\omega - \rho^0)$$

CS emission

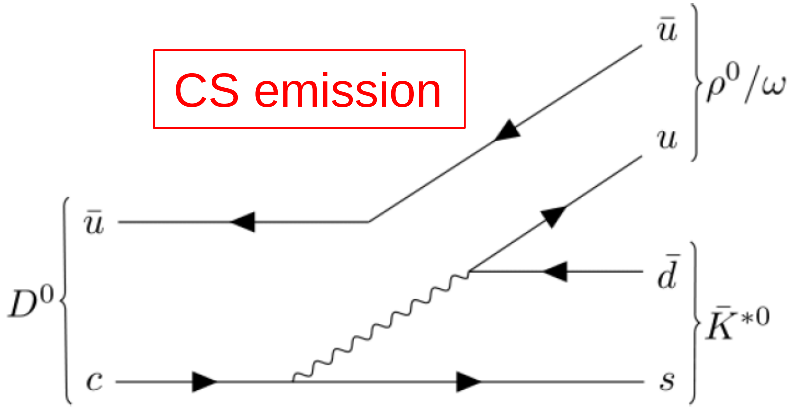

IC transition

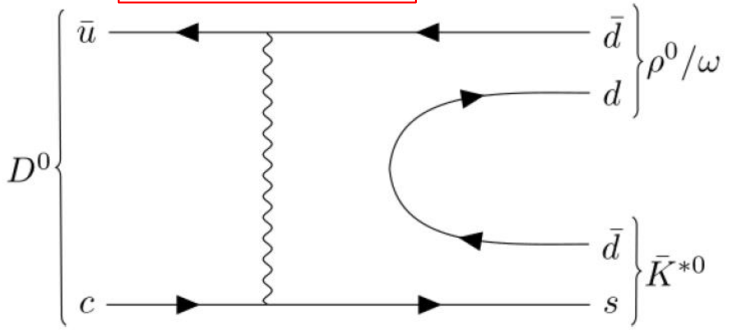

B.R. differences can be possibly accounted for by the interferences between the color suppressed emission (**CS**) and internal conversion (**IC**) transitions.

The CF decay of $D^0 \to K^{*-}\rho^+$ with the direct W emission (DE) has not been precisely measured in experiment!

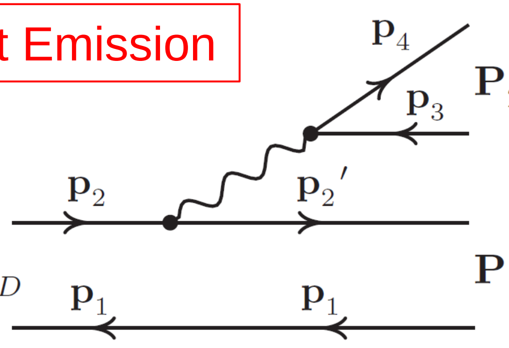

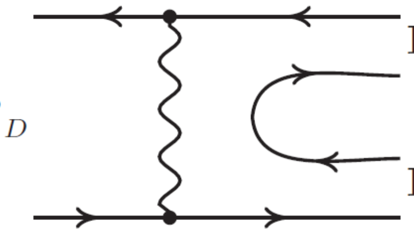

$$BR(D^0 \to K^{*-}\rho^+) = (6.5 \pm 2.5)\ \% \sim 5 \times BR(D^0 \to K^{*0}\rho^0)$$

H. Albrecht et al., New results on D0 decays, Z. Phys. C56, 7 (1992)

Decay channels	Amplitudes
$K^{*-}\rho^+$	$[g_{\rm DE}^{(\rm P)} + e^{i\theta} g_{{\rm IC}(s\bar{d})}^{(\rm P)}]V_{cs}V_{ud}$
$\bar{K}^{*0}\rho^0$	$\frac{1}{\sqrt{2}}[g_{\rm CS}^{(\rm P)} - e^{i\theta} g_{{\rm IC}(s\bar{d})}^{(\rm P)}]V_{cs}V_{ud}$
$\bar{K}^{*0}\omega$	$\frac{1}{\sqrt{2}}[g_{\rm CS}^{(\rm P)} + e^{i\theta} g_{{\rm IC}(s\bar{d})}^{(\rm P)}]V_{cs}V_{ud}$

- The CF decay amplitudes can be parametrized out by topological diagrams for the DE, CS, and IC transitions.
- θ is a trivial phase angle which prefers $\theta = 180°$.

Topological diagram approach (TDA):

Y. Kohara, PRD44, 2799 (1991); L.L. Chau, H.Y. Cheng and B. Tseng, PRD54, 2132 (1996); X.G. He and W. Wang, CPC42, 103108 (2018)

- **Singly Cabibbo suppressed (SCS) decays** $(\sim V_{cs}V_{us}/\,V_{cd}V_{ud})$:

Transition amplitude:

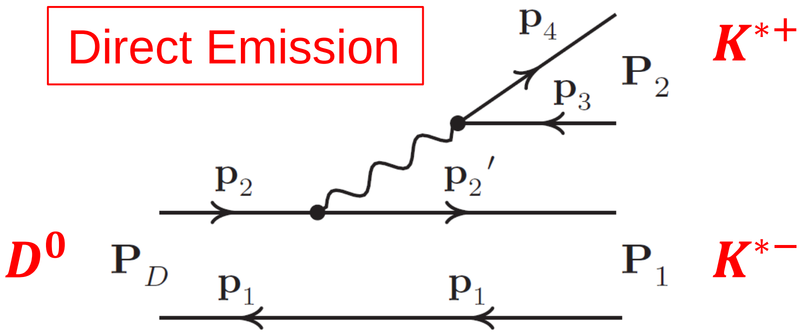

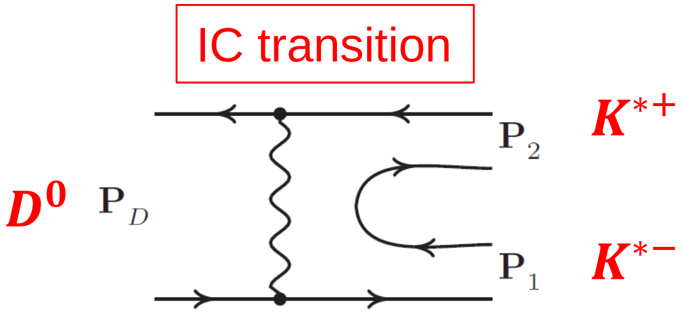

$$[g^{(\mathrm{P})}_{\mathrm{DE}} + e^{i\theta} g^{(\mathrm{P})}_{\mathrm{IC}(s\bar{s})}]V_{cs}V_{us}$$

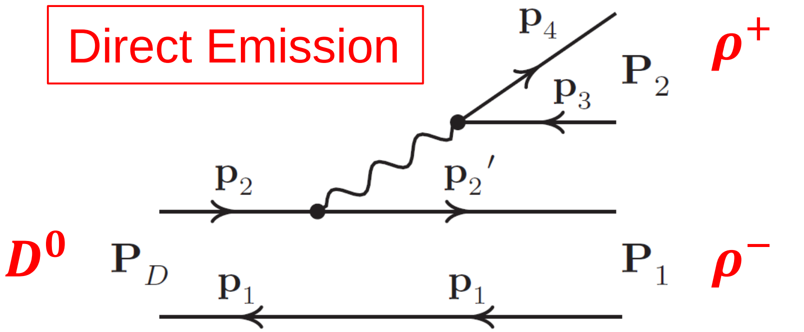

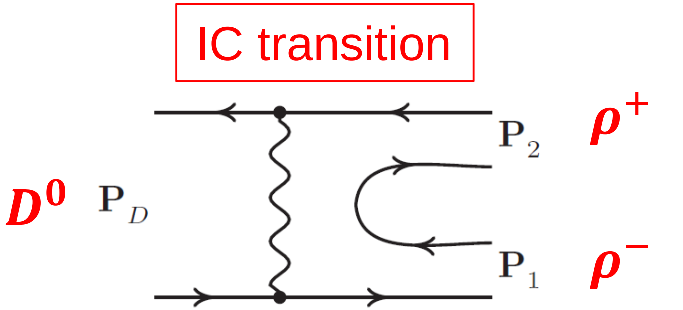

$$[g^{(\mathrm{P})}_{\mathrm{DE}} + e^{i\theta} g^{(\mathrm{P})}_{\mathrm{IC}(d\bar{d})}]V_{cd}V_{ud}$$

The SCS decays of $D^0 \to K^{*+}K^{*-}$ and $\rho^+\rho^-$, which is the only one involving the dominant DE transitions among the SCS decays, have NOT been measured in experiment!

The neutral decay channels involves the CS emissions and IC transitions:

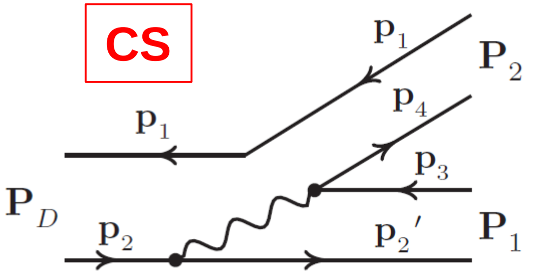

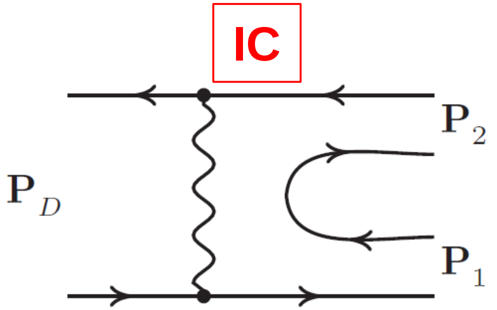

Decay channels	Amplitudes	
$K^{*+}K^{*-}$	$[g^{(P)}_{DE} + e^{i\theta} g^{(P)}_{IC(s\bar{s})}] V_{cs} V_{us}$	DE+IC
$K^{*0}\bar{K}^{*0}$	$e^{i\theta}[g^{(P)}_{IC(s\bar{s})} V_{cs} V_{us} + g^{(P)}_{IC(d\bar{d})} V_{cd} V_{ud}]$	
$\rho^+\rho^-$	$[g^{(P)}_{DE} + e^{i\theta} g^{(P)}_{IC(d\bar{d})}] V_{cd} V_{ud}$	
$\rho^0\rho^0$	$\frac{1}{2}[-g^{(P)}_{CS} + e^{i\theta} g^{(P)}_{IC(d\bar{d})}] V_{cd} V_{ud}$	CS+IC
$\omega\omega$	$\frac{1}{2}[g^{(P)}_{CS} + e^{i\theta} g^{(P)}_{IC(d\bar{d})}] V_{cd} V_{ud}$	
$\rho^0\omega$	$-\frac{1}{2} e^{i\theta} g^{(P)}_{IC(d\bar{d})} V_{cd} V_{ud}$	IC
$\phi\rho^0$	$\frac{1}{\sqrt{2}} g^{(P)}_{CS} V_{cs} V_{us}$	CS
$\phi\omega$	$\frac{1}{\sqrt{2}} g^{(P)}_{CS} V_{cs} V_{us}$	

in unit of ($\times 10^{-3}$)

$K^{*0}\bar{K}^{*0}$	**S**	0.50 ± 0.03[21]
	P	0.27 ± 0.02[21]
	D	0.11 ± 0.01[21]
	T	-
	L	-
	Total	0.88 ± 0.04[21]
$\rho^+\rho^-$	T	-
	L	-
	Total	-
$\rho^0\rho^0$	**S**	0.18 ± 0.13[21]
	P	0.53 ± 0.13[21]
	D	0.62 ± 0.30[21]
	T	0.56 ± 0.07[19]
	L	1.27 ± 0.10[19]
	Total	1.85 ± 0.13[19]
		1.33 ± 0.35[21]
$\omega\omega$	T	-
	L	-
	Total	-
$\rho^0\omega$	T	-
	L	-
	Total	-
$\phi\rho^0$	**S**	1.40 ± 0.12[21]
	P	0.08 ± 0.04[21]
	D	0.08 ± 0.03[21]
	T	-
	L	-
	Total	1.56 ± 0.13[21]
$\phi\omega$	T	0.65 ± 0.10[20]
	L	~ 0 [20]
	Total	0.65 ± 0.10[20]

[19] J. M. Link et al., FOCUS Colla., Phys. Rev. D, 75:052003, 2007

[20] M. Ablikim et al., BESIII Colla., Phys. Rev. Lett., 128(1):011803, 2022

[21] P. d'Argent et al., JHEP, 05:143, 2017

- Notice that there exist significant differences between the $K^{*+}K^{*-}$ and $K^{*0}\overline{K}^{*0}$ channels.

$K^{*+}K^{*-}$	$[g_{\rm DE}^{(\rm P)} + e^{i\theta} g_{{\rm IC}(s\bar{s})}^{(\rm P)}] V_{cs} V_{us}$
$K^{*0}\bar{K}^{*0}$	$e^{i\theta}[g_{{\rm IC}(s\bar{s})}^{(\rm P)} V_{cs} V_{us} + g_{{\rm IC}(d\bar{d})}^{(\rm P)} V_{cd} V_{ud}]$

$$BR\left(D^0 \to K^{*+}K^{*-}\right) \gg BR\left(D^0 \to K^{*0}\overline{K}^{*0}\right)$$

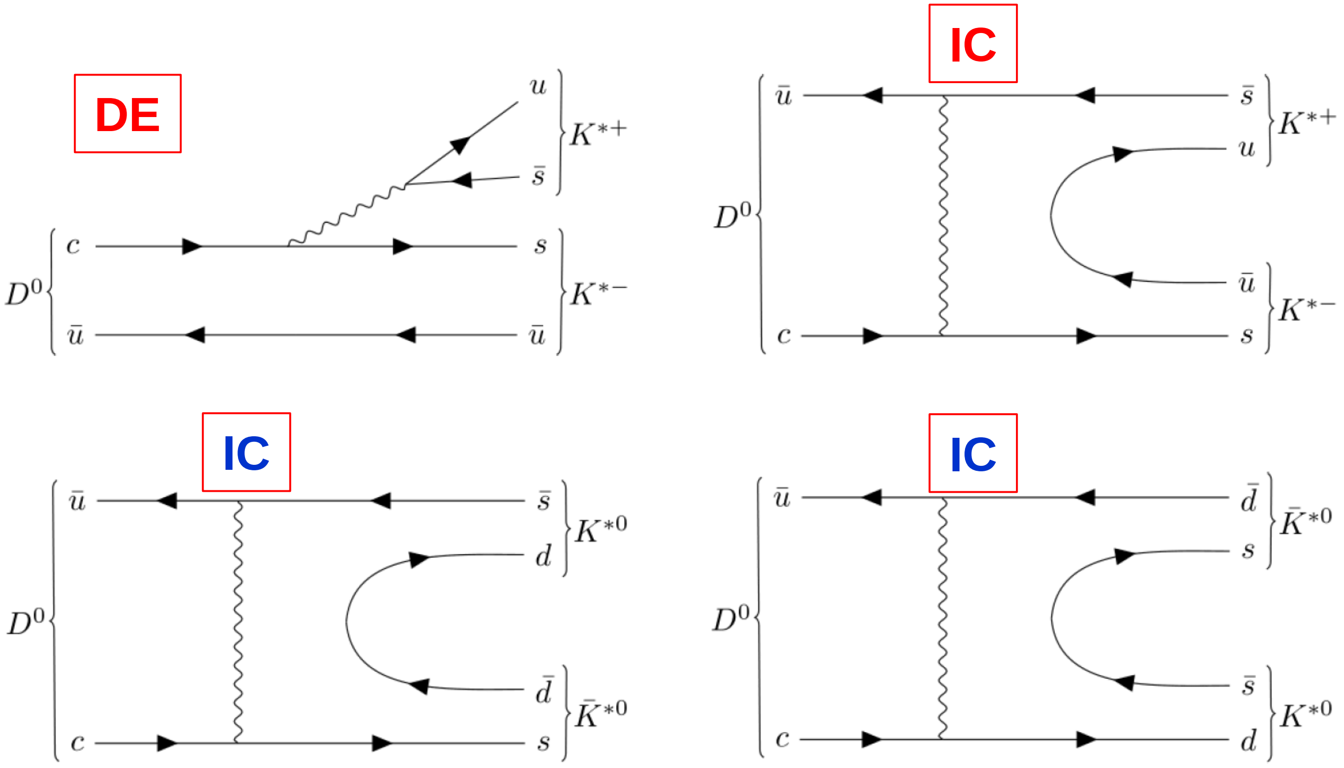

- Long distance transition mechanism due to the $K^*\overline{K}^*$ final-state interactions (FSIs) should be considered:

$$2m_{K^*} \sim m_\phi + m_\rho \sim m_\phi + m_\omega$$

- Moreover, FSIs involving other intermediate meson rescatterings can also contribute. A systematic treatment is required.

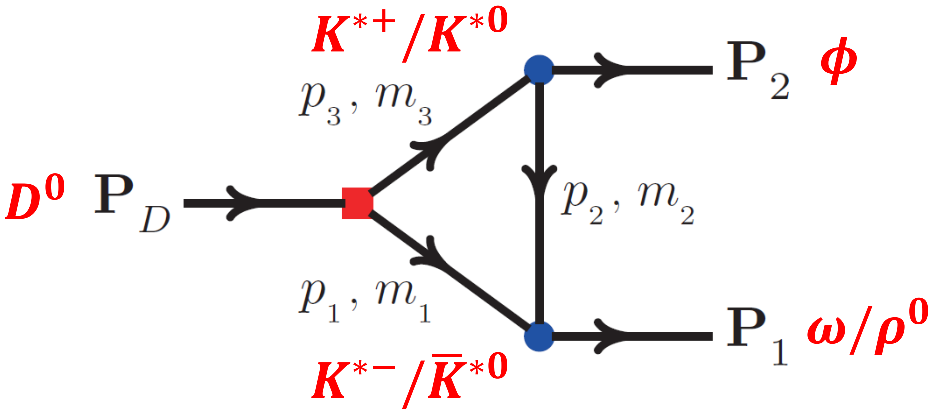

3. Tree-level short-distance transitions vs. long-distance final state interactions

- Taking $D^0 \to \phi\rho^0/\phi\omega$ as an example, the tree-level amplitude reads:

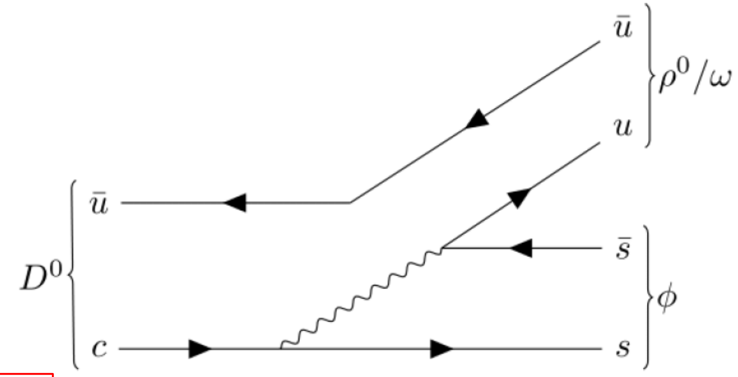

$$i\mathcal{M}_{(\mathrm{P})}(D^0 \to \phi\rho^0/\phi\omega)$$

$$= \langle \phi\rho^0/\phi\omega|\phi(u\bar{u})\rangle\langle\phi(u\bar{u})|H_{W(\mathrm{P})}^{(\mathrm{CS})}|D_0\rangle = \frac{1}{\sqrt{2}} g_{\mathrm{CS}}^{(\mathrm{P})} V_{cs} V_{us}$$

To be calculated explicitly in the NRCQM

- The amplitude due to the intermediate $K^{*+}K^{*-}$ rescatterings can be written as:

$$i\mathcal{M}_{(\mathrm{P})\phi\rho^0}^{loop} = \frac{1}{\sqrt{2}} g_{\mathrm{DE}}^{(\mathrm{P})} V_{cs} V_{us} \sum_{(\mathbb{K})} \tilde{\mathcal{I}}[(\mathrm{P}); K^{*+}, K^{*-}, (\mathbb{K})]$$

$$i\mathcal{M}_{(\mathrm{P})\phi\omega}^{loop} = \left(\frac{1}{\sqrt{2}} g_{\mathrm{DE}}^{(\mathrm{P})} + e^{i\delta} g_{\mathrm{IC}(s\bar{s})}^{(\mathrm{P})}\right) V_{cs} V_{us} \times \sum_{(\mathbb{K})} \tilde{\mathcal{I}}[(\mathrm{P}); K^{*+}, K^{*-}, (\mathbb{K})] ,$$

"P" can be either "PC" or "PV" for parity-conserving or parity-violating amplitudes.

Different strange particle exchanges in $K^{*+}K^{*-} \to \phi\rho^0/\phi\omega$.

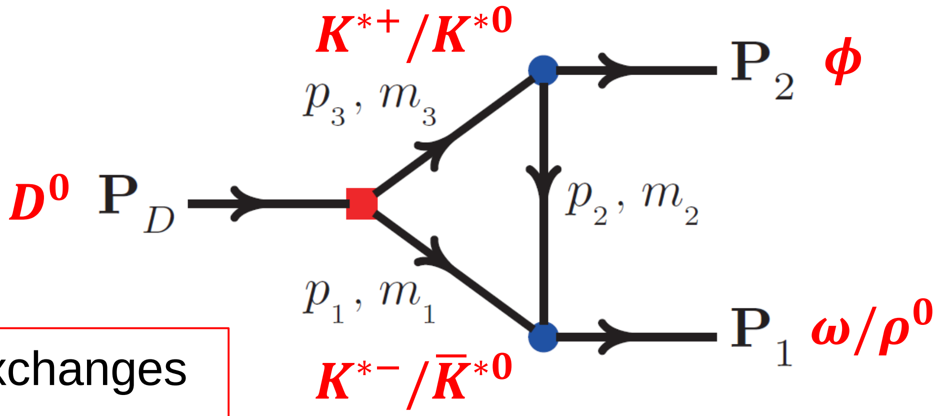

Numerical results in comparison with the data

Leading processes with the DE trans.

CF trans. with CS

SCS trans. with CS

in unit of ($\times 10^{-3}$)

Process		Experiments	b.r.s *with* FSIs	b.r.s *without* FSIs
$K^{*-}\rho^+$	T	-	$57.92^{+0.96}_{-0.59}$	47.59
	L	-	$7.88^{+0.43}_{-0.43}$	4.58
	Total	65.0 ± 25.0[31]	$65.80^{+1.39}_{-1.02}$	52.17
$\bar{K}^{*0}\rho^0$	T	18.0 ± 6.0[18]	$10.95^{+1.28}_{-1.55}$	12.36
	L	-	$4.34^{+1.09}_{-1.09}$	5.31
	Total	15.9 ± 3.5[18] 15.15 ± 0.75 [32]	$15.29^{+2.37}_{-2.64}$	17.68
$\bar{K}^{*0}\omega$	T	-	$6.85^{+0.36}_{-0.51}$	7.52
	L	-	$2.62^{+0.09}_{-0.08}$	2.76
	Total	11.0 ± 5.0[31]	$9.48^{+0.45}_{-0.59}$	10.28
$K^{*+}K^{*-}$	T	-	$6.22^{+0.26}_{-0.37}$	4.02
	L	-	$2.93^{+0.09}_{-0.16}$	1.83
	Total	-	$9.15^{+0.35}_{-0.53}$	5.86
$K^{*0}\bar{K}^{*0}$	**S**	0.50 ± 0.03[21]	$0.56^{+0.25}_{-0.15}$	0.92
	P	0.27 ± 0.02[21]	$0.27^{+0.006}_{-0.009}$	0.30
	D	0.11 ± 0.01[21]	$0.01^{+0.004}_{-0.003}$	0.006
	T	-	$0.58^{+0.13}_{-0.08}$	0.84
	L	-	$0.27^{+0.10}_{-0.07}$	0.39
	Total	0.88 ± 0.04[21]	$0.84^{+0.24}_{-0.15}$	1.23

Decay channels	Amplitudes
$K^{*-}\rho^+$	$[g^{(P)}_{\rm DE} + e^{i\theta} g^{(P)}_{{\rm IC}(s\bar{d})}]V_{cs}V_{ud}$
$\bar{K}^{*0}\rho^0$	$\frac{1}{\sqrt{2}}[g^{(P)}_{\rm CS} - e^{i\theta} g^{(P)}_{{\rm IC}(s\bar{d})}]V_{cs}V_{ud}$
$\bar{K}^{*0}\omega$	$\frac{1}{\sqrt{2}}[g^{(P)}_{\rm CS} + e^{i\theta} g^{(P)}_{{\rm IC}(s\bar{d})}]V_{cs}V_{ud}$
$K^{*+}K^{*-}$	$[g^{(P)}_{\rm DE} + e^{i\theta} g^{(P)}_{{\rm IC}(s\bar{s})}]V_{cs}V_{us}$
$K^{*0}\bar{K}^{*0}$	$e^{i\theta}[g^{(P)}_{{\rm IC}(s\bar{s})}V_{cs}V_{us} + g^{(P)}_{{\rm IC}(d\bar{d})}V_{cd}V_{ud}]$

- The long-distance FSIs are crucial and evident.
- The difference between $\bar{K}^{*0}\rho^0$ and $\bar{K}^{*0}\omega$ indicates the non-negligible contributions from the IC transitions. About 10% corrections from the long-distance FSIs are expected.

Numerical results in comparison with the data

in unit of $(\times 10^{-3})$

Process		Experiments	b.r.s *with* FSIs	b.r.s *without* FSIs
$\rho^+\rho^-$	T	-	$4.19^{+0.31}_{-0.31}$	5.44
	L	-	$0.91^{+0.09}_{-0.04}$	1.36
	Total	-	$5.10^{+0.40}_{-0.35}$	6.81
$\rho^0\rho^0$	**S**	0.18 ± 0.13[21]	$0.38^{+0.42}_{-0.26}$	0.49
	P	0.53 ± 0.13[21]	$0.42^{+0.06}_{-0.06}$	0.23
	D	0.62 ± 0.30[21]	$0.04^{+0.02}_{-0.02}$	0.01
	T	0.56 ± 0.07[19]	$0.67^{+0.28}_{-0.20}$	0.48
	L	1.27 ± 0.10[19]	$0.18^{+0.22}_{-0.14}$	0.25
	Total	1.85 ± 0.13[19] 1.33 ± 0.35[21]	$0.85^{+0.49}_{-0.34}$	0.73
$\omega\omega$	T	-	$0.050^{+0.005}_{-0.004}$	0.019
	L	-	$0.028^{+0.0001}_{-0.002}$	0.00065
	Total	-	$0.078^{+0.005}_{-0.006}$	0.020
$\rho^0\omega$	T	-	$1.03^{+0.01}_{-0.03}$	0.84
	L	-	$0.09^{+0.009}_{-0.004}$	0.13
	Total	-	$1.11^{+0.013}_{-0.024}$	0.97
$\phi\rho^0$	**S**	1.40 ± 0.12[21]	$1.41^{+0.16}_{-0.14}$	0.48
	P	0.08 ± 0.04[21]	$0.07^{+0.03}_{-0.02}$	0.05
	D	0.08 ± 0.03[21]	$0.003^{+0.001}_{-0.001}$	~ 0
	T	-	$1.01^{+0.14}_{-0.12}$	0.37
	L	-	$0.48^{+0.05}_{-0.04}$	0.16
	Total	1.56 ± 0.13[21]	$1.48^{+0.19}_{-0.17}$	0.53
$\phi\omega$	T	0.65 ± 0.10[20]	$0.64^{+0.12}_{-0.10}$	0.34
	L	~ 0 [20]	$0.03^{+0.001}_{-0.002}$	0.15
	Total	0.65 ± 0.10[20]	$0.67^{+0.12}_{-0.10}$	0.49

Leading processes with the DE trans.

CF trans. with CS

SCS trans. with CS

$\rho^+\rho^-$	$[g^{(P)}_{DE} + e^{i\theta} g^{(P)}_{IC(d\bar{d})}] V_{cd} V_{ud}$
$\rho^0\rho^0$	$\frac{1}{2}[-g^{(P)}_{CS} + e^{i\theta} g^{(P)}_{IC(d\bar{d})}] V_{cd} V_{ud}$
$\omega\omega$	$\frac{1}{2}[g^{(P)}_{CS} + e^{i\theta} g^{(P)}_{IC(d\bar{d})}] V_{cd} V_{ud}$
$\rho^0\omega$	$-\frac{1}{2} e^{i\theta} g^{(P)}_{IC(d\bar{d})} V_{cd} V_{ud}$
$\phi\rho^0$	$\frac{1}{\sqrt{2}} g^{(P)}_{CS} V_{cs} V_{us}$
$\phi\omega$	$\frac{1}{\sqrt{2}} g^{(P)}_{CS} V_{cs} V_{us}$

- Without the long-distance FSI contributions it is impossible to account for the difference between the $\phi\rho^0$ and $\phi\omega$ decays.
- The suppression of the $\omega\omega$ channel indicates the relative strength between the CS and IC transitions.
- The $\rho^0\omega$ channel is dominantly driven by the IC transition for which the experimental measurement will provide a direct constraint on this mechanism.

4. Summary

- The limitation of QM is unsurprising.
- Rich spectra can arise from the multiquark scenario. In contrast, the hadronic molecule scenario provides an economic solution.
- Apart from the hadron spectroscopy, threshold dynamics play a crucial role for understanding many newly observed phenomena in various processes.
- Theoretical tools bridging the quark and hadron D.O.F. are still required.
- Systematic studies of the threshold effects need inputs from experimental data.

Thanks for your attention!

Exotics of Type-III:
Peak structures caused by kinematic effects, in particular, by triangle singularity.

$$\Gamma_3(s_1, s_2, s_3) = \frac{1}{i(2\pi)^4}\int \frac{d^4q_1}{(q_1^2 - m_1^2 + i\epsilon)(q_2^2 - m_2^2 + i\epsilon)(q_3^2 - m_3^2 + i\epsilon)}$$
$$= \frac{-1}{16\pi^2}\int_0^1\int_0^1\int_0^1 da_1\, da_2\, da_3\, \frac{\delta(1 - a_1 - a_2 - a_3)}{D - i\epsilon},$$

$$D \equiv \sum_{i,j=1}^{3} a_i a_j Y_{ij}, \quad Y_{ij} = \frac{1}{2}\left[m_i^2 + m_j^2 - (q_i - q_j)^2\right]$$

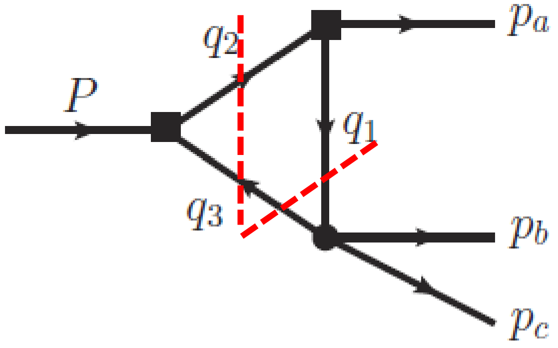

The **TS** occurs when all the three internal particles can approach their on-shell condition simultaneously:

$$\partial D/\partial a_j = 0 \quad \text{for all j=1,2,3.} \quad \Rightarrow \quad \det[Y_{ij}] = 0$$

L. D. Landau, Nucl. Phys. 13, 181 (1959);
J.J. Wu, X.-H. Liu, Q. Zhao, B.-S. Zou, Phys. Rev. Lett. 108, 081003 (2012);
Q. Wang, C. Hanhart, Q. Zhao, Phys. Rev. Lett. 111, 132003 (2013); Phys. Lett. B 725, 106 (2013)
X.-H. Liu, M. Oka and Q. Zhao, PLB753, 297(2016);
F.-K. Guo, C. Hanhart, U.-G. Meissner, Q. Wang, Q. Zhao, B.-S. Zou, arXiv:1705.00141[hep-ph], Rev. Mod. Phys. 90, 015004 (2018) ; F.-K. Guo, X.-H. Liu and S. Sakai, Prog. Part. Nucl. Phys. 112, 103757 (2020)
M.-C. Du and Q. Zhao, PRD 104, 036008 (2021); PRD 100, 036005 (2019); Y. Cheng, L. Qiu, and Q. Zhao, PRD in press, arXiv:2407.10234

$e^+e^- \to \eta J/\psi$

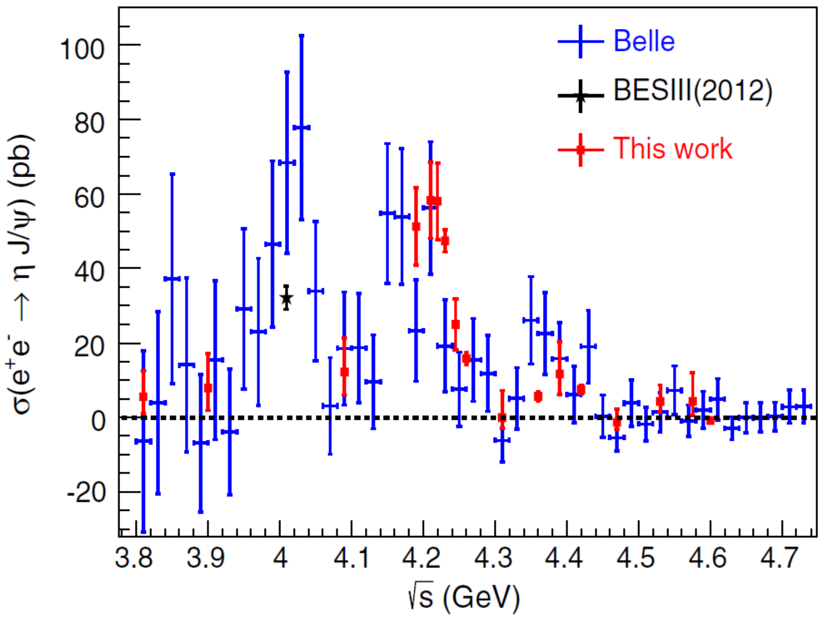

BESIII, PRD91, 112005 (2015)

$e^+e^- \to \eta J/\psi$

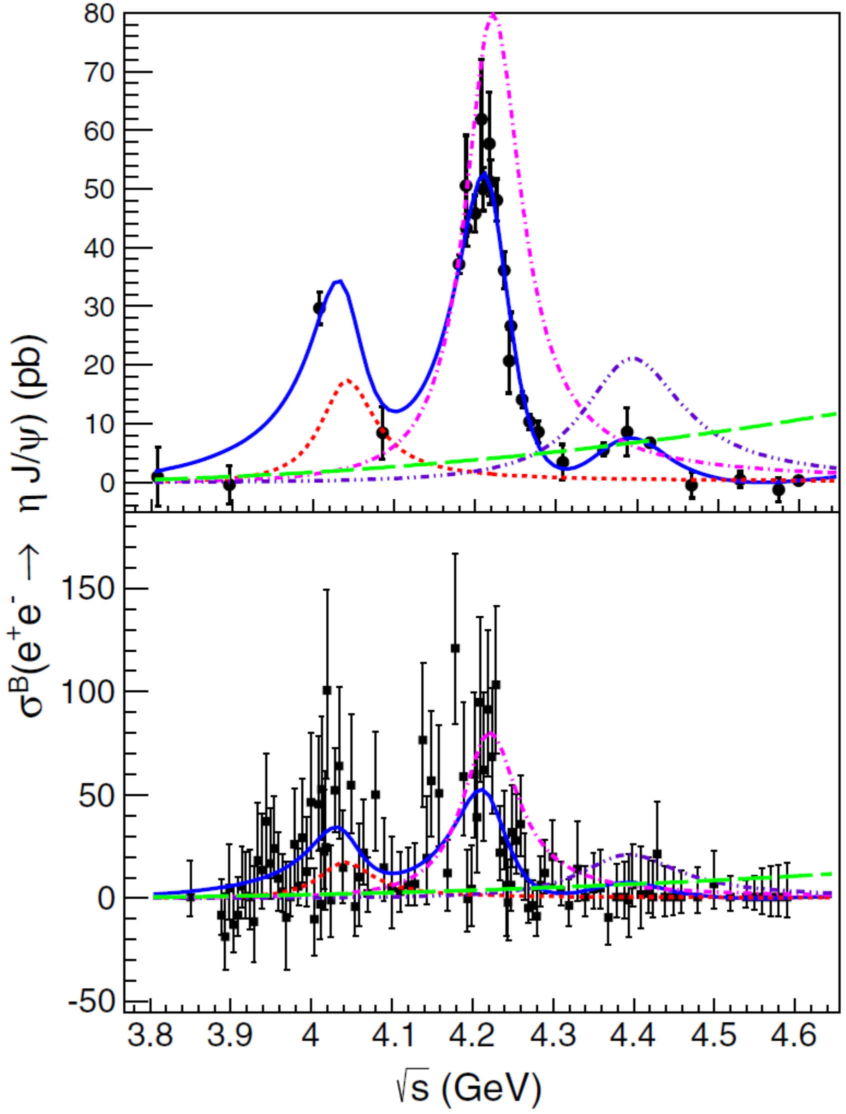

BESIII, PRD102, 031101 (2020)

$e^+e^- \to \eta\psi(2S)$

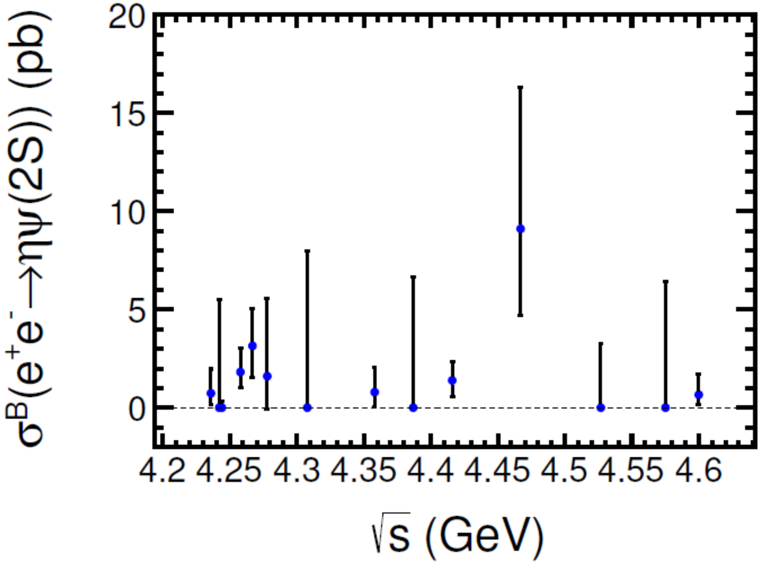

BESIII, *JHEP* 10 (2021) 177

$e^+e^- \to \eta' J/\psi$

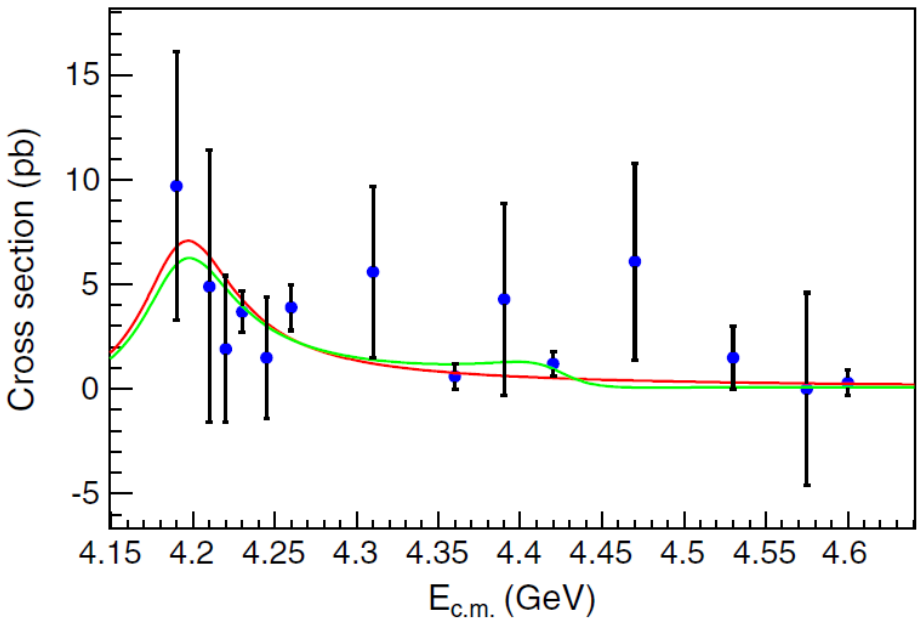

BESIII, PRD94, 032009 (2016)

$e^+e^- \to \eta' J/\psi$

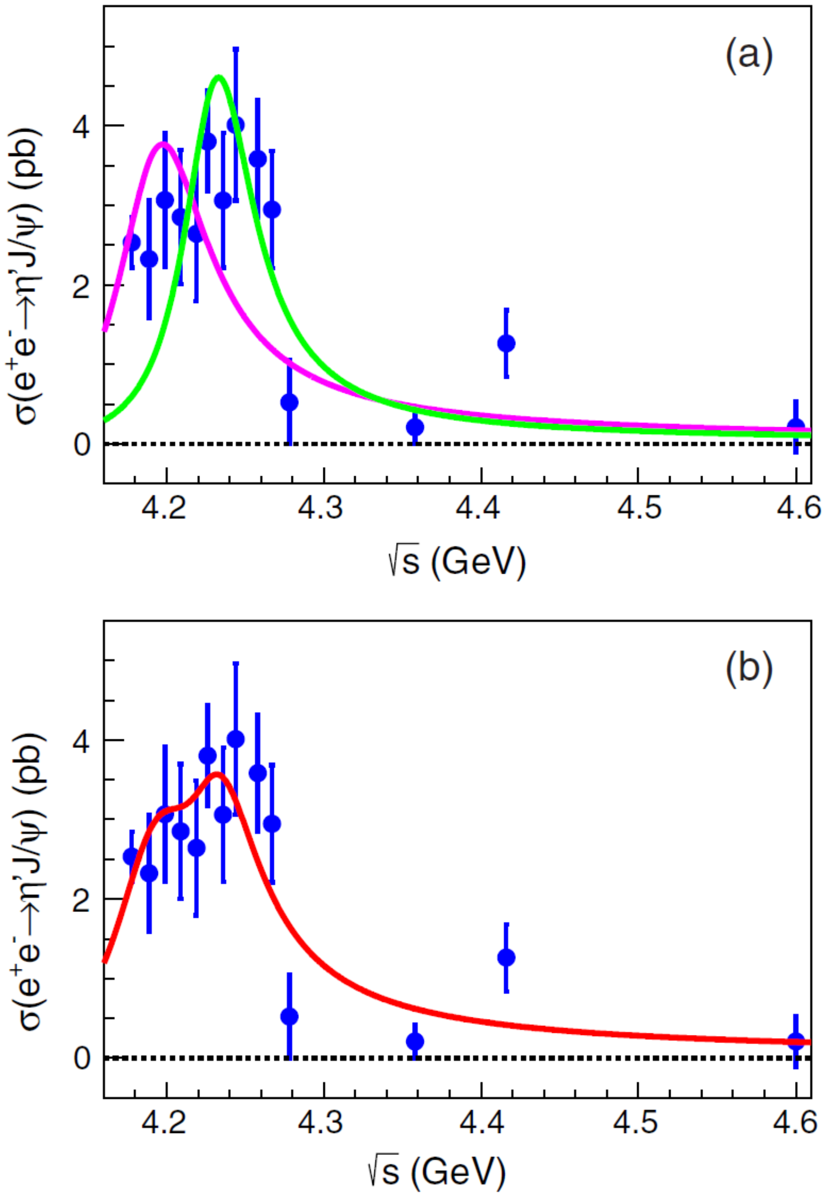

BESIII, PRD101, 012008 (2020)

$e^+e^- \to \pi^+\pi^-\psi(3686)$

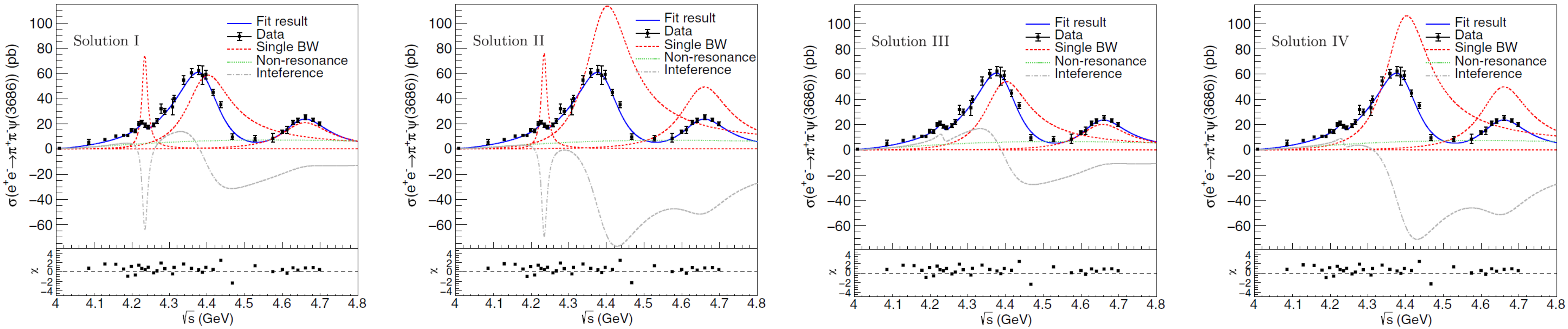

Parameters	Solution I	Solution II	Solution III	Solution IV
$\mathrm{M}(Y4220)$ (MeV/c^2)	4234.4 ± 3.2			
$\Gamma^{\mathrm{tot}}(Y4220)$ (MeV)	17.6 ± 8.1			
$\mathcal{B}\Gamma^{ee}(Y4220)$ (eV)	1.59 ± 0.75	1.63 ± 0.78	0.02 ± 0.01	0.02 ± 0.01
$\mathrm{M}(Y4390)$ (MeV/c^2)	4390.3 ± 6.0			
$\Gamma^{\mathrm{tot}}(Y4390)$ (MeV)	143.3 ± 10.0			
$\mathcal{B}\Gamma^{ee}(Y4390)$ (eV)	10.70 ± 4.13	20.72 ± 2.46	9.86 ± 4.11	19.44 ± 2.04

Phys.Rev.D 104 (2021) 5, 052012; arXiv:2107.09210[hep-ex]

Phys.Rev.D 104 (2021) 5, 052012; arXiv:2107.09210[hep-ex]

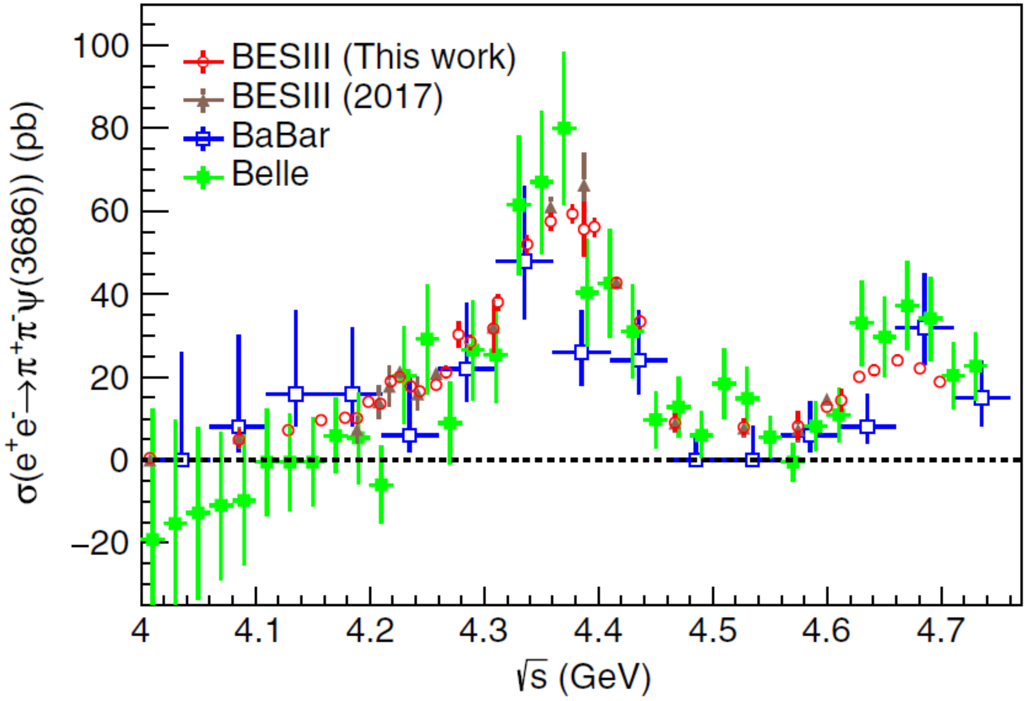

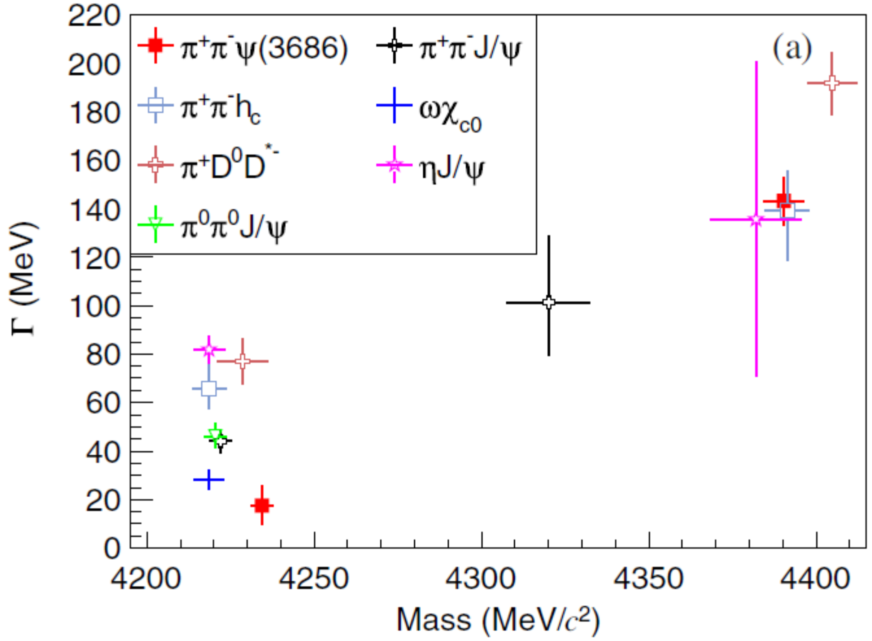

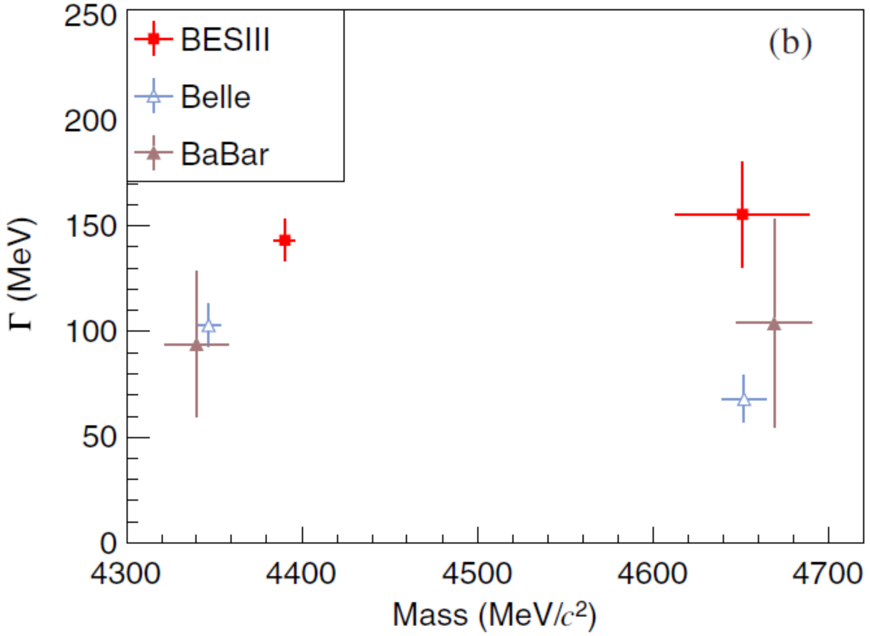

BESIII, *Phys.Rev.D* 104 (2021) 9, 092001

$e^+e^- \to \gamma\chi_{cJ}$

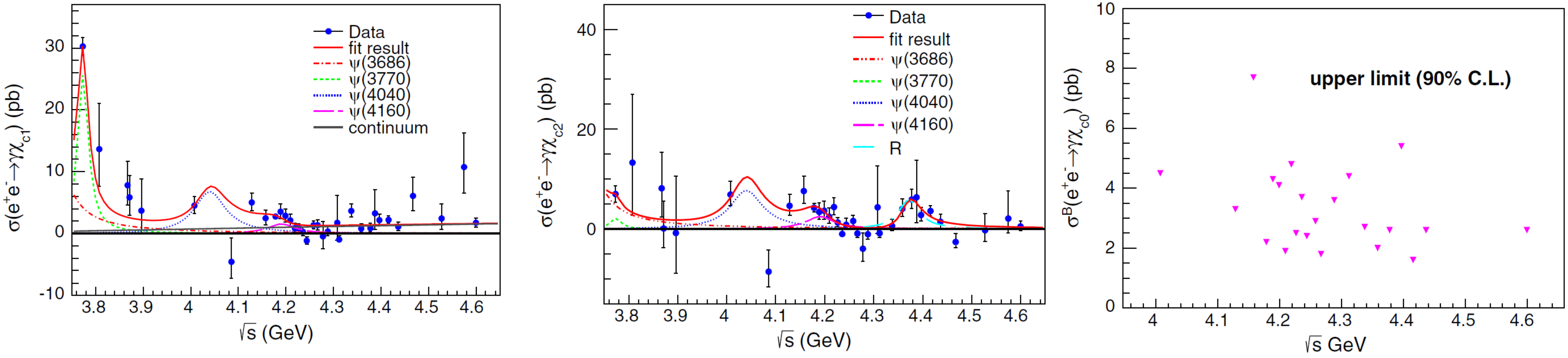

TABLE II. Results of the fit to the $e^+e^- \to \gamma\chi_{c2}$ cross sections. The unit of the e^+e^- partial width is eV/c^2. The errors are statistical only.

Parameter	Solution I	Solution II	Solution III	Solution IV
$\Gamma^{ee}\mathcal{B}(\psi(3770) \to \gamma\chi_{c2})$	$(0.6 \pm 0.4) \times 10^{-1}$			
$\Gamma^{ee}\mathcal{B}(\psi(4040) \to \gamma\chi_{c2})$	$(13.4 \pm 4.7) \times 10^{-1}$	$(6.9 \pm 3.5) \times 10^{-1}$	$(13.3 \pm 4.7) \times 10^{-1}$	$(6.9 \pm 3.5) \times 10^{-1}$
$\Gamma^{ee}\mathcal{B}(\psi(4160) \to \gamma\chi_{c2})$	$(6.8 \pm 1.9) \times 10^{-1}$	$(2.1 \pm 0.9) \times 10^{-1}$	$(6.4 \pm 1.8) \times 10^{-1}$	$(2.1 \pm 0.9) \times 10^{-1}$
$M(\mathcal{R})$	4371.7 ± 7.5			
$\Gamma^{\mathrm{tot}}(\mathcal{R})$	51.1 ± 17.6			
$\Gamma^{ee}\mathcal{B}(\mathcal{R} \to \gamma\chi_{c2})$	$(4.7 \pm 1.6) \times 10^{-1}$	$(3.9 \pm 1.3) \times 10^{-1}$	$(4.4 \pm 1.5) \times 10^{-1}$	$(4.1 \pm 1.4) \times 10^{-1}$
ϕ_1	$241.5° \pm 15.0°$	$105.6° \pm 33.7°$	$238.9° \pm 14.8°$	$107.3° \pm 34.2°$
ϕ_2	$248.7° \pm 31.3°$	$24.8° \pm 39.2°$	$252.6° \pm 31.7°$	$19.5° \pm 30.8°$